ISSN 8755-6839

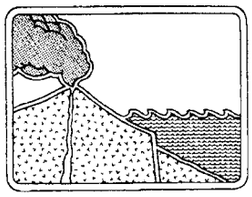

SCIENCE OF
TSUNAMI HAZARDS

The International Journal of The Tsunami Society

Volume 20 **Number** 4 **Published Electronically** 2002

SECOND TSUNAMI SYMPOSIUM PAPERS - II

OBJECTIVE: **The Tsunami Society** publishes this journal to increase and disseminate knowledge about tsunamis and their hazards.

DISCLAIMER: Although these articles have been technically reviewed by peers, **The Tsunami Society** is not responsible for the veracity of any statement, opinion or consequences.

Submit manuscripts of articles, notes or letters to the Editor. If an article is accepted for publication the author(s) must submit a scan ready manuscript, a TeX or a PDF file in the journal format. Issues of the journal are published electronically in PDF format. The journal issues for 2002 are available at

http://www.sthjournal.org.

Tsunami Society members will be advised by e-mail when a new issue is available and the address for access. There are no page charges or reprints for authors.

Previous volumes of the journal are available in PDF format at

http://epubs.lanl.gov/tsunami/

and on a CD-ROM from the Society to Tsunami Society members.

ISSN 8755-6839 **http://www.sthjournal.org**

Published Electronically by The Tsunami Society in Honolulu, Hawaii, USA

LOCALLY GENERATED TSUNAMIS IN HAWAII: A LOW COST, HEAL TIME WARNING SYSTEM WITH WORLD WIDE APPLICATIONS

Daniel A. Walker
Haleiwa, Hawaii USA
Robert K. Cessaro
PTWC, Honolulu, Hawaii USA

ABSTRACT

Cellular runup detectors have been installed along those coastlines of the island of Hawaii that have been frequently inundated by locally generated tsunamis. These devices provide for near instantaneous (i.e., less than 1 minute) warnings of locally generated tsunamis. Principal components of the detectors are cellular transceivers and water sensors. Because of the extensive use of these devices throughout the security industry, they are extremely reliable and cost effective. Such instruments could be useful in the measurement of tsunami runups in coastal areas of the world with cellular coverage. As satellite versions of the cellular transceivers become available, eventual coverage areas threatened by tsunamis, storm surges, and flash floods may be possible.

INTRODUCTION

In the pre-dawn hours of 29 November 1975, a locally generated tsunami struck a remote camping area on the southeastern coast of the Big Island. The maximum wave height at the Halape campgrounds (Figure 1) was estimated to be 26 feet (7.9 m). Just to the east, at Keauhou Landing, the wave height was estimated to be 47 feet (14.3 m). Within minutes the waves generated by this 7.2 Ms Kalapana earthquake were striking the western shores of the Big Island with runups of up to 11 feet (3.4 m). Two lives were lost at Halape. Many more could have been killed or injured if the tsunami occurred several hours later or if the maximum runups occurred in heavily populated areas. A nearly identical tsunami in terms of runup size and distribution occurred in 1868 (Figure 2). In addition, the Big Island has experienced other locally generated, potentially destructive tsunamis (Table 1; Figure 3). For this reason state and county civil defense agencies in Hawaii recently began sponsoring renewed investigations of the risks posed by local tsunamis, and possible methods for improving warnings for those tsunamis.

One conclusion of these investigations was that a Kalapana type of earthquake and tsunami on the Kona Coast would not only be devastating to that coast, but would be dangerous to other coastlines throughout the State (Fryer and Watts, 2001; Mader, 1988; Mader 2001). Futhermore, an analysis of the historical data revealed that a majority of large Big Island earthquakes did not produce significant tsunamis. In the twentieth century 16 of the 19 earthquakes with surface wave magnitudes of 6.0 or greater did not generate any reported tsunamis (Walker, 1999). Also, potentially destructive tsunamis were generated by small earthquakes or submarine landslides (Table 1). The 1952 tsunami (10 feet or 3m) was generated by a 4.5 Ms earthquake. The tsunamis of 1901 (4 feet or 1.2m) and 1919 (14 feet or 4.3m) were probably generated by submarine landslides. There were no reports in newspapers of felt earthquakes at those times. For the 1919 event, a potentially destructive tsunami with a 1Cfoot (4.3 m) runup at Milolii traveled northward to Kailua where a runup of 8 feet (2.4 m) was measured. No earthquake was reported by the Hawaiian Volcano Observatory which should have had seismographs in operation at that time.

All of these observations suggest that warnings should be called for: (a) only the largest of earthquakes, preferably with the recording of significant tsunamis on tide gauges or other water level recorders; and, (b) any earthquake with accompanying significant recordings on tide gauges or other wave recorders. Unfortunately, most of the coastal areas of the Big Island are not suitable for the deployment of conventional wave recorders, Such instruments are expensive to purchase, install, and maintain; and require sheltered harbors. In those coastal areas of the Big Islandwhere locally generated tsunamis are most likely to originate (i.e., from Kaimu southward to South Point and up the Kona Coast to Kailua), there are only two reasonably sheltered harbors (i.e., Keauhou and Kailua) and one marginally sheltered harbor at Milolii.

DISCUSSION

Ideally, as a practical alternative, low cost, low maintenance, reliable tsunami detectors could be widely distributed on land along those low-lying coastal areas of the Big Island most likely to be struck by locally generated tsunamis. Installation ofjust such an array of detectors was completed in 2001, and is the topic of the following discussions.

Cellular Runup Detectors

Cellular Runup Detectors (CRD's) were installed on Civil Defense siren poles at Punaluu, Honuapo, Milolii, Napoopoo, Kahaluu Beach Park, Pahoehoe Beach Park, the Old Kona Airport just north of Kailua, and on a post attached to a warehouse at Honaunau just south of Napoopoo. Each CRD consists of a sensor box, transmitter box, solar panel, and antenna unit. The base of the sensor box is mounted about 1 foot (0.3 m) above the ground, the transmitter box is about 10 feet (3 m) above the ground, and the solar panel and antenna unit are just above the transmitter box. The height of the sensor units above sea level at the above mentioned sites ranges from 8 to 14 feet (2.4 to 4.3m), and the distance inland from the shoreline ranges from 60 to 390 feet (lg.3 to 118.9 m).

The sensor unit consists of an outer stainless steel weatherproof box, an inner plastic box, and the sensor. The outer stainless steel box has a hole in its bottom that is covered with stainless steel wire and shade cloth to discourage rats, mice, lizards, ants, and other insects from entering. As the box is mounted close to the ground, the hole can only be seen by putting one's head on the ground and by looking up at the bottom of the box a few inches away. The box also has a padlock. Inside the sensor box is a plastic box with two large holes covered by shade cloth to further deter insects and small animals. The sensor unit is located inside the plastic box. The sensor is a wallet-sized piece of epoxy with four stainless steel pins protruding slightly out of the epoxy block in its corners. These sensors are used extensively throughout the security industry to detect flooding in homes or businesses. A wire also comes out of the sensor and is routed into a conduit that runs out of the bottom of the sensor box and up to its relay and power supply unit in the transmitter box. Holes in the back of the sensor box permit mounting with stainless steel lag screws onto the wooden siren poles. The box has a beveled and hooded face plate that can be removed by loosening two screws and the padlock. The only possible way for the sensor box to be flooded is by water rising up from below the unit, The dimensions of the sensor box are 6 in X 4 in X 8 in (15 cm X 10 cm X 20 cm).

The transmitter box has a waterproofing gasket, with access by removal of its padlock and 12 screws from the front panel. In the unlikely event of a gasket failure, the box is designed to channel water away from its interior. Mounted onto the inside back of the box is a thick plastic cutting board. This served as a platform for several components. These include the sensor's relay and power supply unit, the solar panel regulator, a timer box, the cell phone transceiver, wiring, and a terminal block for routing of the wires, The cell phone transceiver is widely used throughout the security industry to alert central station receivers of undesirable changes in ambient conditions (e.g.; fires, flooding,

break-ins, equipment malfunctions, high or low temperatures, etc.). Sitting in the bottom of the transmitter box is a 38 amp-hour battery. Three silicon rubber sealed conduit holes come out of the bottom of the box. One goes to the solar panel, another to the antenna, and the third is for the sensor unit cable from the sensor box. Brackets on the top, bottom, and side of the box permit mounting with lag screws or banding materials. The dimensions of the transmitter box are 12 in X 9 in X 24 in (30 cm X 23 cm X 61 cm).

The solar panels used on the Big Island were either 20 or 30 watts depending on the available sunlight at the site. The antenna was the standard antenna that came with the cellular transceiver. It had to be unscrewed from its unit and placed in a PVC pipe mounted on the pole above the transmitter box. This was necessary because the antenna could not function inside the stainless steel transmitter box.

Performance

All of the units were installed in 2001 - a test unit at the Richard H. Hagemeyer Pacific Tsunami Warning Center (PTWC) in June; and on the Big Island, four units in August and four units in September. Thus far there have been no false warnings received at PTWC from these units; and, in more than a hundred tests of flooding the sensors, alarms at PTWC have always been triggered. A solar panel was stolen, and two 20-watt panels were found to be too small to sustain a charge on their batteries. They were replaced with 30-watt panels. In the entire operation thus far, the only failure was a bad solar panel voltage regulator. The time required to trigger the alarm on the central station receiver at PTWC once flooding is initiated on a Big Island sensor is generally about 25 seconds.

Software and Messages

The OH-2000 is the central station alarm receiver that accepts runup detector alarms reports over a standard phone line. The unit is supplied as a standard rack mount unit, powered by 120VAC and a 12V standby battery. Up to 16 phone lines may be connected to standard telephone jacks located on the back of the unit. Digital communication, with the OH-2000, is performed over an RS-232 connection. An 80 column printer may also be connected to the parallel printer port. Programming options and updates may be accessed via the programming serial port.

The automation software, *ohcom*, handles *Contact ID* messages as described in the *OH-2000 Instruction* Manual. Receipt of critical messages, such as flooding and low battery, are indicated on the graphical user interface (GUI). All messages are logged to monthly log files. The OH-2000 sends a *heartbeat* message every 30 seconds, which toggles an indicator on the *ohcom* GUI. If *ohcom* fails to receive a heartbeat from the OH-2000 the GUI displays a failure mode graphic. *Ohcom* also provides a software activity. These indicators may be used in combination to evaluate the software and OH-2000 communication state.

The *ohcom* GUI is composed of a coastline map of the island of Hawaii along with labeled symbols for the installed runup detectors and a few geographic reference points. Ohcom responds to flooding, power condition and weekly tests from the central site in Atlanta. As an added safety measure, a trigger module is installed with each detector,to

provide daily contact closure on channel 4. If ohcom fails to receive a daily trigger Tom a runup detector, the associated symbol on the GUI will change color to grey. Detection of a power discrepancies or failure of the weekly test is indicated by a yellow symbol until corrected. All abnormal conditions are accompanied by an email condition report to the operator. Nominal runup detector condition is indicated by a green symbol. On receipt of a flooding message, the GUI symbol will turn red and a digital page will be sent to the on-duty personnel.

Future Applications

Improved versions of the cellular transceiver now have the capability to trigger sirens attached to other units at other sites. This has important implications for coastal areas at risk, but not yet serviced by warning sirens. Also, satellite phone versions of the CRD's have the potential for substantial worldwide reductions in the fatalities and injuries associated with locally generated tsunamis, storm surges, and flash floods.

CONCLUSIONS AND RECOMMENDATIONS

The eight detectors now in place should provide warnings of locally generated tsunamis to most of the population of the Big Island as well as, if necessary, the rest of the State. No local warning system is perfect, however, in that some fatalities may be unavoidable in those coastal areas struck by a tsunami before a detector has been flooded. This would most likely occur along the southeastern coast between Kapoho and Punaluu. There is a tide gauge at Kapoho and a CRD at Punaluu, but nothing in between. Should a tsunami occur in this area, people at Kapoho, Ahalanui, Pohoiki, Kaimu, in the coastal campground areas of the National Park, at Punaluu, Honuapo, and Ka Lae (South Point) would have little or no warnings. Therefore a detector should be installed at Apua Point, approximately midway between Kaimu and Punaluu. This should be done as soon as possible because the Kaimu to Punaluu region, although sparsely populated, is the area of the Big Island most likely to be struck by a locally generated tsunami. The Apua Point site was tested in February 2002 with a portable system. The flooding was detected at PTWC in about 25 seconds. The area is gently sloping and capable of detecting tsunamis as small as 10 feet without being subjected to false warnings from heavy surf. A detector at this site could provide several minutes of warning to people at Kapoho, Ahalanui, Pohoiki, Kaimu, Punaluu, Honuapo, and Ka Lae. Apua Point is just to the east of Keauhou Landing. Also, consideration should be given to having sirens at other sites within the Hawaii Volcanoes National Park using the new cellular transceiver that can trigger sirens attached to transceivers at other sites. Other coastal campgrounds or frequently visited areas in or near the park include Kaimu, Keauhou Landing, Halape, and Kaaha.

Acknowledgments. Support for this project was provided by funds allocated to the State of Hawaii through NOAA's National Tsunami Hazard Mitigation Program. Our thanks to Hawaii's State and County Civil Defense Agencies for their proactive, responsible actions in supporting this effort.

Note. For information on specifications and current pricing, the following is a list of available web sites for manufacturers of the components used in the construction of the detectors.

Cellular transceiver - Uplink DigiCell 1500, uplink.com, available through adilink.com.
Central station receiver - Osborne-Hoffman OH-2OOO,osbome-hoffmancorn.
Photovoltaic controller - Specialty Concepts ASC 12/4-A, specialtyconceptscom.
Sealed battery - Yuasa NP 38-12, generally available, also through adilink.com.
Solar panels - Solarex MSX20 and MSX30, generally available, also at solarexcom.
Stainless steel instrument boxes - generally available from local sheet metal fabricators.
Timer unit - Stealth Laboratories , stealthlabs.com.
Water sensor - Winland WB-200 Water-Bug, Winland Electronics, winland.com.

REFERENCES

Cox, D. C., and .I. Morgan (1977). Local Tsunamis and Possible Local Tsunamis in m, HIG-77-14, Hawaii Inst. of Geophysics, 118 pp.

Fryer, G. J., and P. Watts (2001). Locally generated tsunamis in Hawaii, http://www.soest.hawaii.edu/tsunami/.

Lander, J. F., and P. A. Lockridge (1989). United States Tsunamis (including United States possessions) 1690-1988, National Geophysical Data Center, Publication 41-2, Boulder, Colorado, 265 pp.

Mader, C. L. (1988). Numerical Modeling of Water Waves, University of California Press, 206 pp.

Mader, C. L. (2001). HILAND OR WALKERK in http://tl4web.lanl.gov/Staff/clmi tsunami.mve/tsunami.htm; or log onto http://www.mccohi.com.

Walker, D. A. (1999). Issues related to local tsunamis in Hawaii, Sci. of Tsunami Hazards, 17-2, 71-84.

Walker, D. A. (2000). Twentieth century Ms and Mw values as tsunamigenic indicators for Hawaii, Sci. of Tsunami Hazards, l&2,69-76.

Daniel A. Walker
Storm and Tsunami Flood Gauges
59530 Pupukea Rd.
Haleiwa, Hi. 96712
walker@hawaii.rr.com

Robert K. Cessaro
Richard H. Hegemeyer Pacific Tsunami Warning Center
91-270 Fort Weaver Rd.
Ewa Beach, Hi. 96706
cessaro@ptwc.noaa.gov

Table 1

Locally Generated Tsunamis in the Twentieth Century*

Ye=	Mo	Dav	MS	Runups or Tide Gauge Readings
1901	08	09	--	4 Il(1.2m) Hoopuloa, Kailua-Kona; obs. Hookena, Honuapo; O.lm Honolulu
1908	09	21	6.8	4 ft (1.2m) Hilo
1919	10	02	--	14 ft (4.3m) Hoopuloa; 8 ft(2.4m) Keauhou; 3 ft (0.9m) Kailua-Kona
1951	08	21	6.9	4 ft (1.2m) Hookena; 3 ft (0.9m) Kailua-Kona, Napoopoo, Milolii; <O.lm Hilo, Honolulu, Port Allen
1952	03	17	4.5	10 ft (3.0m) Kalapana
1975	11	29	7.2	47 ft (14.3m) Keauhou Landing; 1 ft(0.4m) Kahului; O.lm Nawiliwili; <O.lm Coconut Island on Oahu, Honolulu; obs. Lahaina, Hana; many other runups on the Big Island

* All data are taken from Lander and Lockridge (1989). See Walker (2000) for a discussion of the 1901 event. All available data are given unless otherwise indicated. Maui sites are Lahaina, Kahului, and Hana. Kauai sites are Port Allen and Nawiliwili. Newspaper articles were examined for indications of felt earthquakes possibly associated with the 1901 and 1919 events (Cox and Morgan, 1977; and Walker, 2000). None were found.

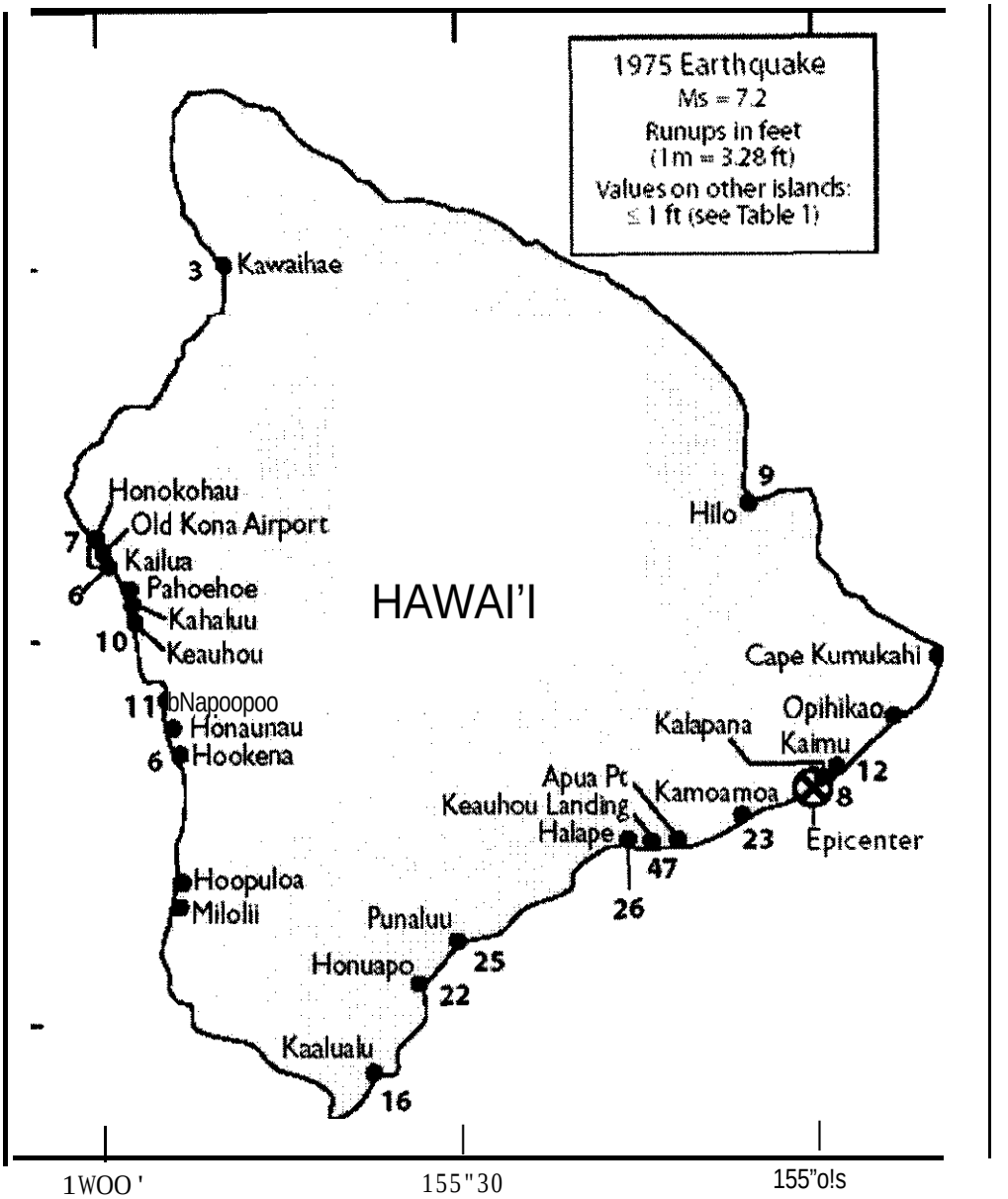

Figure 1. Runup values in feet for the 1975 tsunami as taken from Lander and Lockridge (1989).

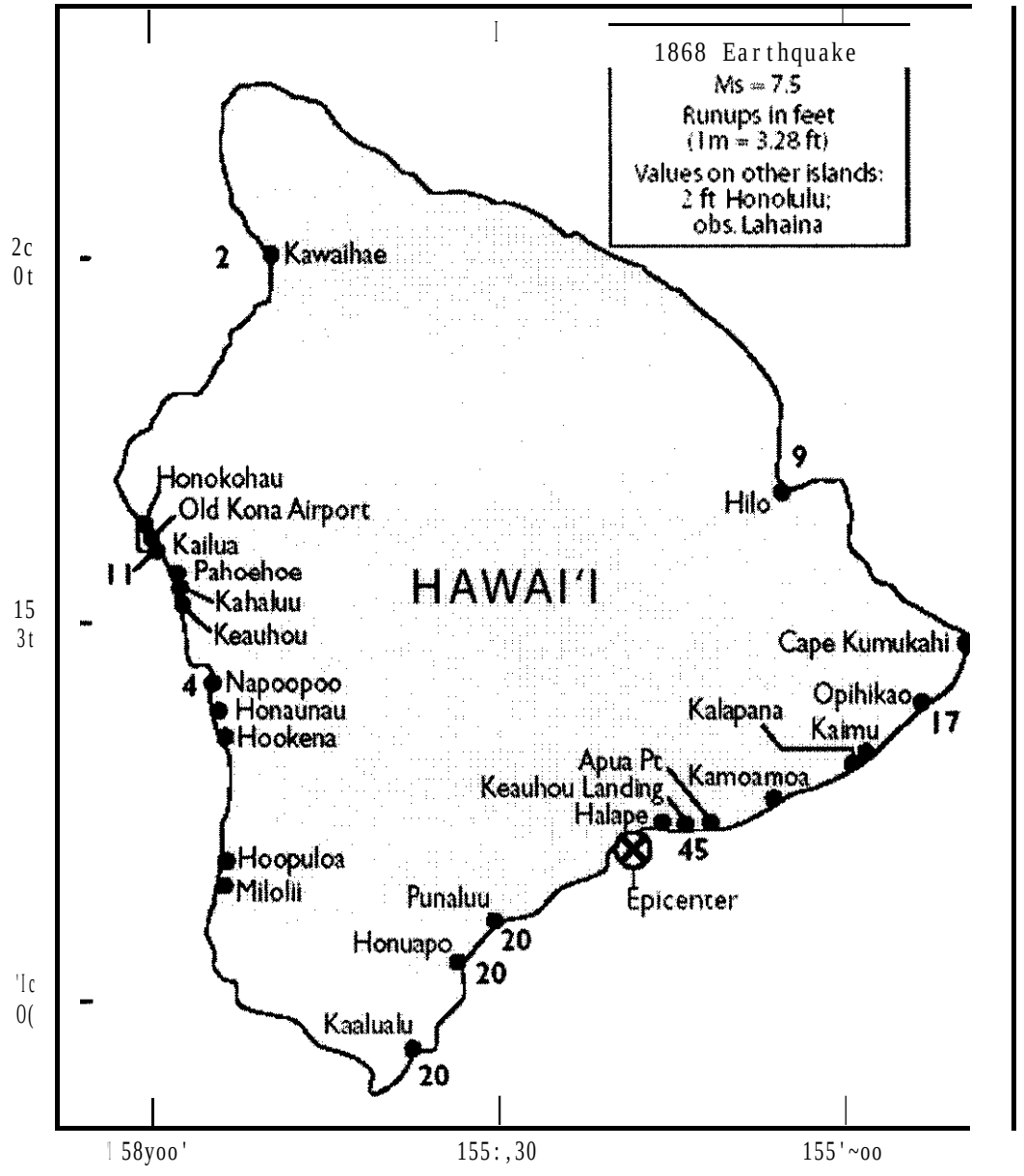

Figure 2. Runup values in feet for the 1868 tsunami. In addition, there are reports of the tsunami being "observed" at other Big Island locations. A value of 7 feet indicated for Apua, may not be consistent with reports that all of the houses in the area were washed away. It should be noted that the waves could have been much larger as they swept across this extensive low-lying point of land. There may have been no topographic features in the area capable of providing evidence of higher elevations. A similar scenario may have occurred further to the east at Kealakomo near Kamoamoa (see Lander and Lo&ridge, 1989).

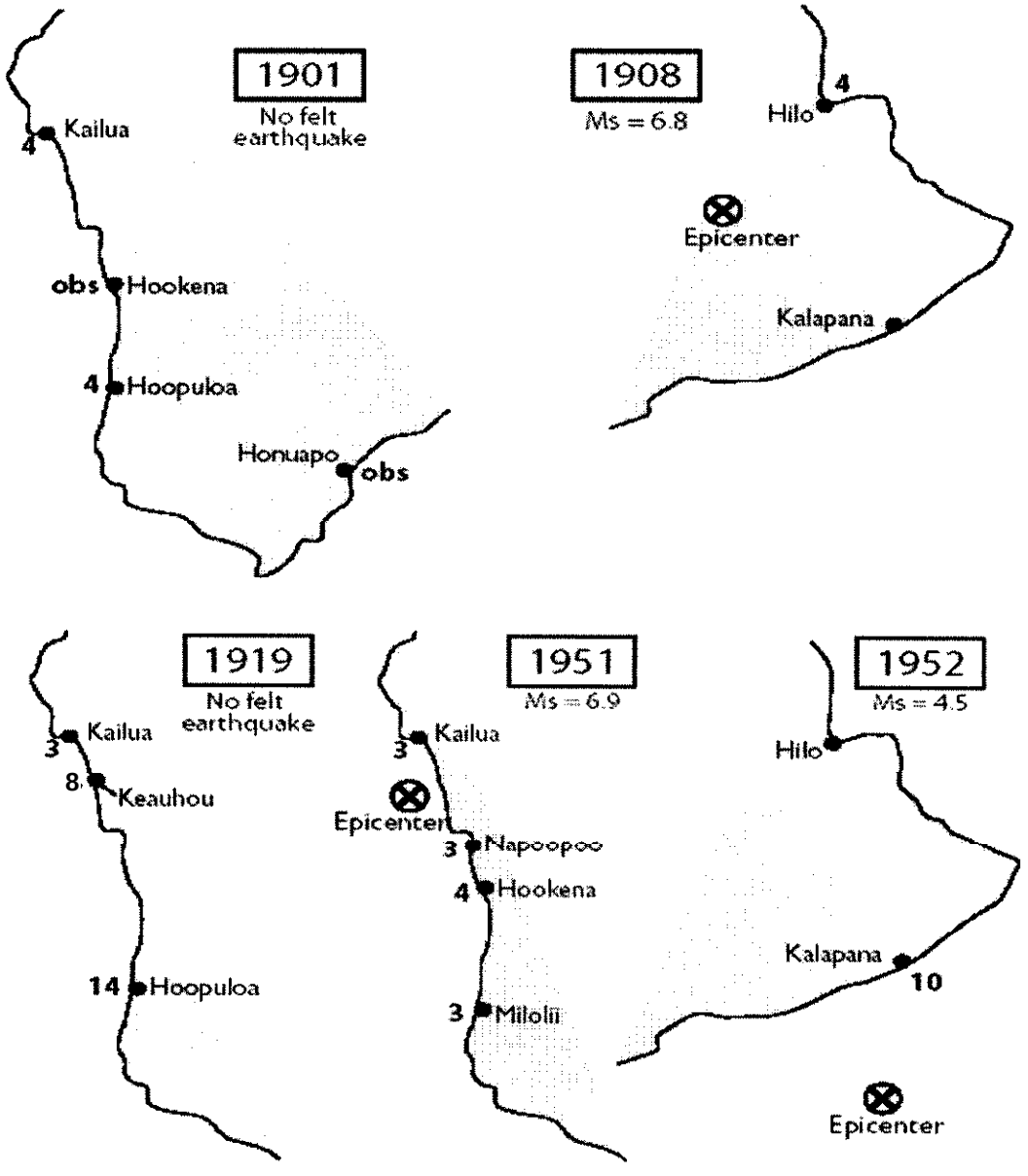

Figure 3. Runup values in feet for other tsunamis in the twentieth century. In newspaper articles discussing the 1901 and 1919 tsunamis, there were no reports of any felt earthquakes that might be associated with these tsunamis. There were also no reports of any instrumentally recorded earthquakes by the Hawaiian Volcano Observatory which was in operation at the time of the 1919 tsunami. The 1901 tsunami was reported to have moved progressively southward from Kailua and around to Honuapo. The only other reported observation for this tsunami was O.lm in Honolulu. The 1951 tsunami was reported to be less that 0.1 m in Hilo, Honolulu, and Port Allen There are no other reported observations for these tsunamis (Lander and Lo&ridge, 1989).

MAGNITUDE-DEPENDENT CORRECTION FOR MWP

Paul M. Whitmore, West Coast/Alaska Tsunami Warning Ctr./NOAA/NWS, Palmer, AK, USA

Seiji Tsuboi, Institute for Frontier Research on Earth Evolution, Yokosuka, Japan

Barry Hirshorn, Pacific Tsunami Warning Center/NOAA/NWS, Ewa Beach, Hawaii, USA

Thomas J. Sokolowski, West Coast/Alaska Tsunami Warning Ctr./NOAA/NWS, Palmer, AK, USA

ABSTRACT

The P-wave moment magnitude, $M_{wp,}$ is shown to have a magnitude-dependent bias when compared to the Harvard CMT M_w. M_{wp} results for 416 earthquakes are compared to the Harvard M_w. In general, M_{wp} is higher than the Harvard M_w for earthquakes less than magnitude 6.8 and lower for those over 6.8. Results are considered consistent enough to add a linear correction based on the initial M_{wp} determination. Based on a linear best fit to the data, the following correction is applied: $M_{wp\ corrected} = (M_{wp\ initial} - 1.03) / 0.843$.

INTRODUCTION

M_{wp} (Tsuboi, *et al*., 1995, Tsuboi, *et al*., 1999) is utilized at both U.S. tsunami warning centers, the Richard H. Hagemeyer Pacific Tsunami Warning Center (PTWC) and the West Coast/Alaska Tsunami Warning Center (WC/ATWC), as it is the fastest method to determine a reasonable estimate of a large earthquake's moment magnitude. The faster an earthquake's size is determined, the sooner tsunami warning centers can issue critical information to emergency managers. Since the M_{wp} technique was developed in 1995, the U.S tsunami warning centers have been testing M_{wp} results, and have been utilizing the method as a supplementary sizing technique using either the original method (Tsuboi, *et al*., 1995) or the later technique (Tsuboi, *et al*., 1999).

M_{wp} was initially developed by Tsuboi, *et al*. (1995) to determine moment magnitudes based on the integrated P-wave displacement waveform for shallow, regional earthquakes in Japan. The scale was extended by Tsuboi, *et a*l. (1999) for earthquakes of any depth and distances up to 100°. To briefly summarize the technique used in this report, M_{wp} is calculated from P-waves recorded on the vertical component of broadband seismometers. The P-wave section of the displacement seismogram, including the pP contribution, is integrated. The first peak, or the first peak and trough, of this integrated seismogram is used to determine the seismic moment from the formula

$$M_o = Max(|\, p_1 \,|, |\, p_1 - p_2 \,|)\frac{4\pi\rho\alpha^3 r}{F^P}, \qquad (1)$$

where M_o is the seismic moment, p_1 and p_2 are the first peak and trough values on the integrated displacement seismogram, ρ and α are the density and P-wave velocity along the propagation path (ρ=3.4x10^{3}kg/m^3, α=7.9km/s), r is the epicentral distance, and F^P is the radiation pattern. M_{wp} is computed from (1) by using the standard moment magnitude formula, $M_w = (\log M_o - 9.1)/1.5$, where M_o is in N·m, and adding 0.2 to the M_w as explained by Tsuboi, *et al*. (1995) to account for F^P. Equation (1) is used to compute M_{wp} at the WC/ATWC. The technique from Tsuboi, *et al*. (1995) is used at PTWC. The techniques are the same, except that only $|p_1|$ is used in the earlier technique.

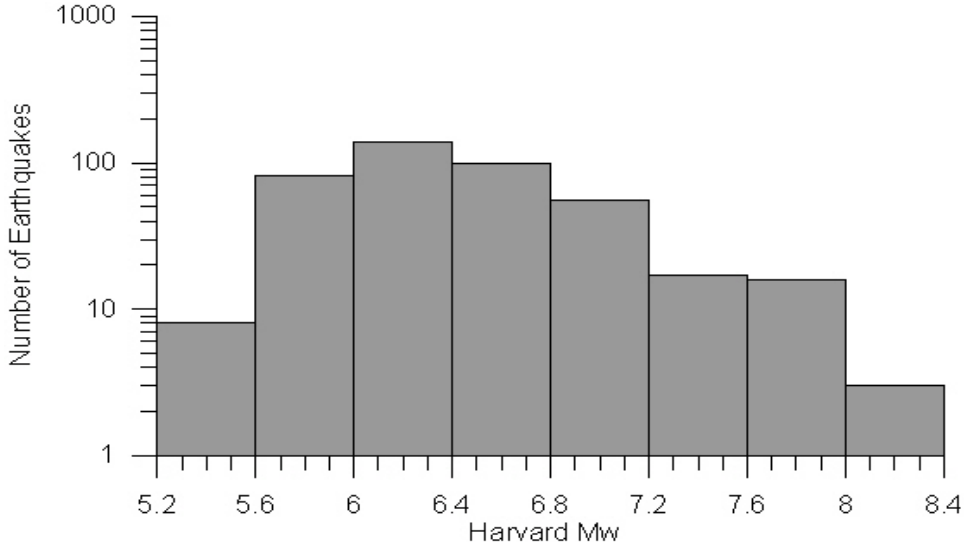

Figure 1. Magnitude distribution of earthquakes used in this study.

With increased numbers of broadband seismometers recorded at the tsunami warning centers, M_{wp} computations can be made more rapidly after earthquake onset, and are more accurate due to the averaging requirements of the technique. To date, over 400 earthquakes have been recorded at the warning centers which were recorded by a sufficient number of broadband seismometers to produce an average M_{wp}. These M_{wp} results have been compared to the Harvard CMT M_w (Dziewonski, *et al.*, 1981), and to epicentral distance and depth to determine if there are any clear M_{wp} trends in relation to those control variables. A definite trend is observed when M_{wp} are compared to the Harvard CMT M_w. The purpose of this study is to examine the magnitude-dependent bias of M_{wp}, and to define a correction so that the initial moment magnitudes issued by the tsunami warning centers are as accurate as possible.

DATA

Seismic data used in this study are obtained from vertical, broadband seismometers recorded at the U.S. tsunami warning centers. The unfiltered velocity signal is integrated to produce a displacement seismogram for up to 120s after the P-onset. The displacement seismogram is integrated again, and this trace is evaluated to determine the first main peak and trough for use in equation (1). Two integrations of the raw velocity data are necessary for this technique, so it is very susceptible to influence by long period noise or DC offset. The signal is not deconvolved to remove instrument response as this may enhance long period noise on broadband seismometers with relatively low long period response corner frequencies and earthquakes with moderate or low signal-to-noise ratios. To prevent underestimating the magnitude due to instrument response, signal from seismometers with flat velocity response to periods beyond 300s is preferred, though results from instruments with flat velocity response to 100s are also included.

Signals from 416 earthquakes between December, 1995 and December, 2001 are evaluated. The earthquakes range from Harvard CMT M_w 5.4 to 8.4 with the majority in the range from 5.6 to 7.2 (Figure 1). The number of recordings used to determine an average M_{wp} ranged from a minimum of three at the beginning of the study to over 40 in the later years. Earthquakes of all hypocentral depths are included and recordings from stations of epicentral distance up to 100^o are used.

RESULTS

Figure 2 displays the average M_{wp} deficit for each earthquake (M_{wp} deficit = Average M_{wp} - M_w HRV) as a function of the Harvard M_w. The average M_{wp} is computed by removing individual M_{wp} results greater than one standard deviation of the difference from the overall M_{wp} average and re-averaging. The standard deviation of the deficit is 0.20 units and the deficit average is 0.03. Figure 2 indicates that the M_{wp} deficit decreases with increasing Harvard M_w. Figure 3 displays average M_{wp} versus the Harvard M_w. A linear, least-squares fit to the data points is also shown and is defined by: Average M_{wp} = (0.843 * M_w HRV) + 1.03. Figure 4 displays the M_{wp} deficit as a function of epicentral distance for individual M_{wp} determinations. Figure 5 displays average M_{wp} deficit as a function of hypocentral depth.

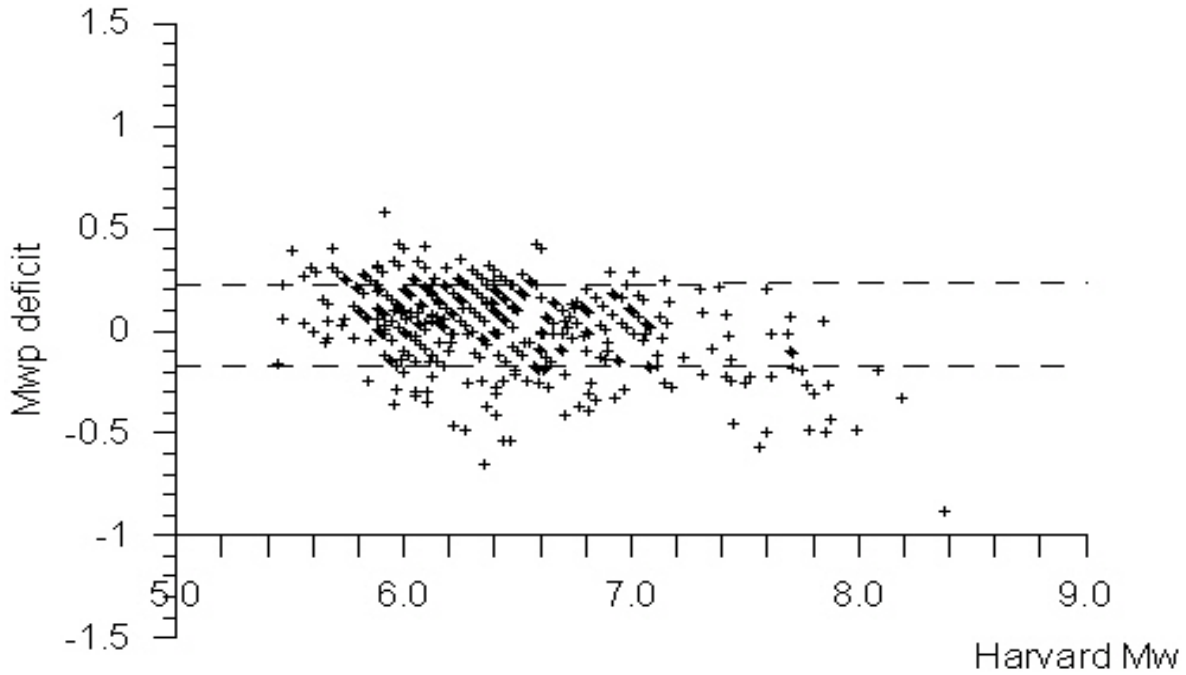

Figure 2. M_{wp} deficit (M_{wp} deficit = Average M_{wp} - M_w HRV) plotted as a function of the Harvard CMT M_w. Average M_{wp} results are plotted for 416 earthquakes. A trend of decreasing deficit with increasing M_w is apparent. The dashed lines represent the standard deviation of the deficit. The overall M_{wp} deficit average is 0.03.

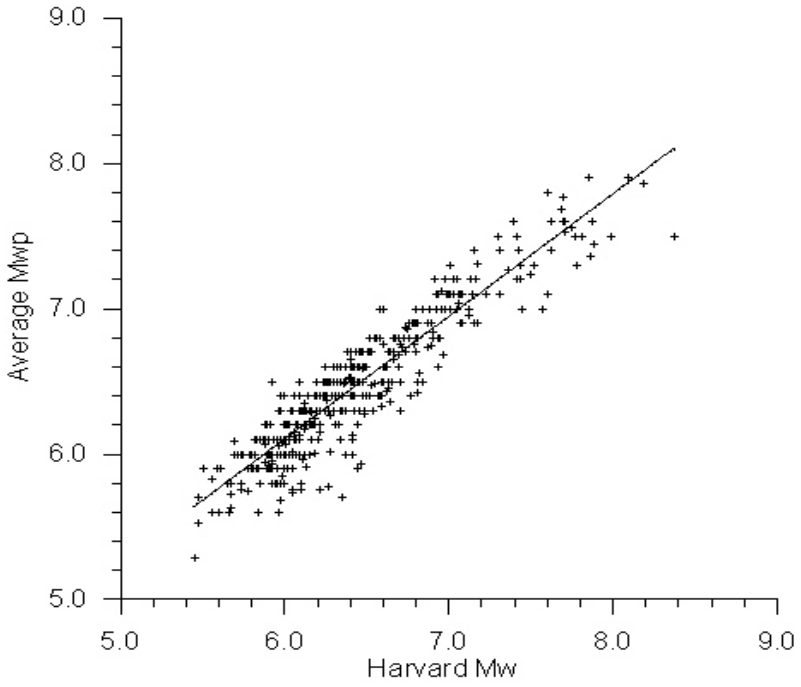

Figure 3. Average M_{wp} plotted as a function of the Harvard CMT M_w. Solid line is the linear, least-squares fit to the data (Average M_{wp} = 0.843 * M_w HRV + 1.03). The 6/23/01 M_w 8.4 Peru earthquake is notably underestimated by M_{wp}; possibly due to the multiple-event nature of this earthquake.

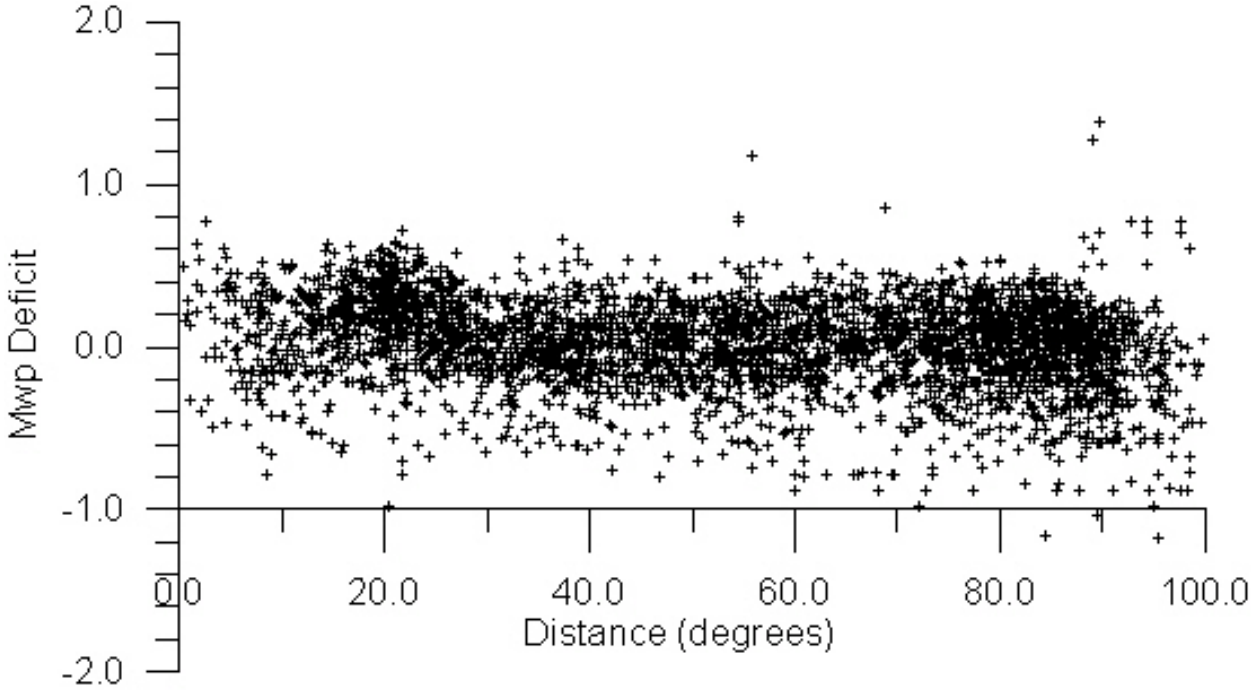

Figure 4. M_{wp} deficit plotted as a function of epicentral distance. M_{wp} deficit is shown for 3748 individual determinations. These individual readings are used to produce the averages shown in the other figures (including those that are eliminated in the re-averaging scheme).

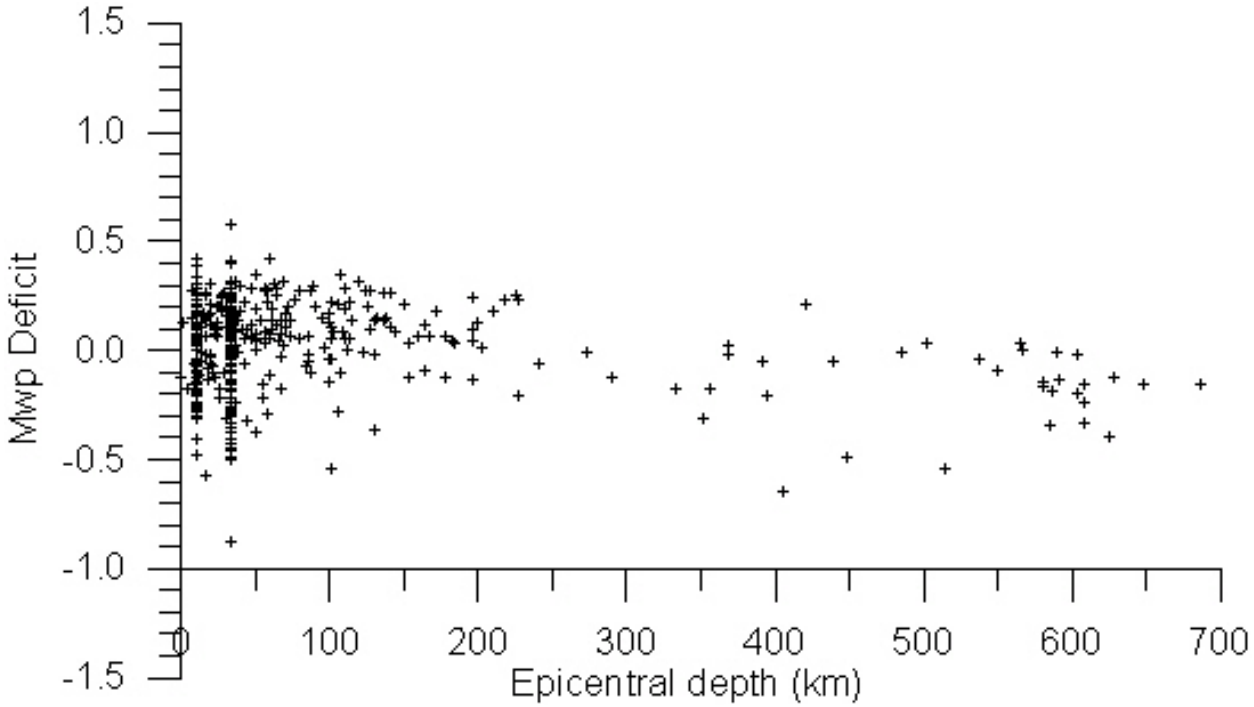

Figure 5. Average M_{wp} deficit plotted as a function of hypocentral depth for 416 earthquakes.

DISCUSSION

No obvious M_{wp} deficit trend is apparent when compared to epicentral distance. However, M_{wp} results appear to be less reliable at distances over 90^o. Also, an increase in the M_{wp} deficit is observed at epicentral distances in the range from 15^o to 25^o.

While the number of earthquakes in this study with hypocentral depth greater than 200km is small compared to the number of shallow earthquakes, a decrease in the M_{wp} deficit with depth is observed. This effect is likely due to the pP phase arriving outside the integration window at these depths which decreases the peak/trough difference in equation (1).

Good agreement between average M_{wp} and Harvard M_w is verified by the 0.03 deficit average. The magnitude-dependent trend shown in Figure 2 can be eliminated in practice by applying a correction based on the linear, least-squares fit to the data. The correction, $M_{wp\ corrected} = (M_{wp\ initial} - 1.03) / 0.843$, is applied to individual M_{wp} computations.

Several factors could be involved in the M_{wp} deficit decrease for large earthquakes. Even with the use of broadband seismometers, the band-limited nature of recorded P-waves may result in saturation of M_{wp}. Also, large earthquakes often are multiple events. M_{wp} may be the size of just one of the sub-events. Regardless of the cause of M_{wp}'s magnitude-dependent bias, the correction proposed here should improve M_{wp} accuracy.

REFERENCES

Dziewonski, A.M., T.-A. Chou, and J.H. Woodhouse (1981). Determination of earthquake source parameters from waveform data for studies of global and regional seismicity, *J. Geophys. Res.,* **86,** 2825-2852.

Tsuboi, S., K. Abe, K. Takano, and Y. Yamanaka (1995). Rapid determination of M_w from broadband P waveforms, *Bull. Seism Soc. Am.,* **83**, 606-613.

Tsuboi, S., P. M. Whitmore, and T. J. Sokolowski. Application of M_{wp} to deep and teleseismic earthquakes, *Bull. Seism Soc. Am.,* **89**, 1345-1351.

A PRELIMINARY ASSESSMENT OF TSUNAMI HAZARD AND RISK IN THE INDONESIAN REGION

Jack Rynn
Centre for Earthquake Research in Australia
PO Box 276, Indooroopilly,, Brisbane, Queensland 4068, Australia

ABSTRACT

The natural hazard of tsunami has, for too long, been underrated as a potential cause of major disasters. However, several devastating tsunamis in and around the Pacific Ocean Basin over the last decade - all claiming significant loss of life, major property and environmental damage and severe socio-economic losses - have heightened the awareness of this natural hazard. As a consequence, significant mitigation strategies and measures in tsunami-prone regions of the world (such as the Pacific Basin, Mediterranean Region, Atlantic Ocean) have been undertaken in recent years. However, for the high tsunami risk Indonesian Region, a more considered approach needs to be addressed.

Indonesia is a region with a considerable record of tsunami occurrence dating back hundreds of years. In a large number of these instances, devastating effects have been repotted. However, reliable and complete data bases, scientific analyses and integration of relevant information into disaster planning have been lacking. This paper reviews the status of available tsunami information (with particular reference to Indonesian and Japanese studies and the recently published Historical Tsunami Data Base for the US Pacific Coast UTDBIUS). presents a comprehensive data base (the central element to any tsunami hazard assessment) for the period 2000BC through 2001AD in the approximate region 9ON to IO'S, 104"E to 140"E and reviews available quantitative hazard and risk assessments. Comments are made on the integration of such assessments to the reduction of community vulnerability and to the prevention of potential damage (risk management) to major commercial development projects for the Indonesian region.

INTRODUCTION

The Indonesian region is a very complex and violent tectonic zone on the Earth's surface in relation to the geological evolutionary processes (known as plate tectonics). Several tectonic plates converge herein, as evidenced by subduction zones, major faults, volcanoes and other geological processes. This tectonic situation is manifested in the natural hazards of earthquake, volcanic eruptions and collateral hazards of landslide and tsunami. The historical record, at least for the past 2000 years, documents the frequent and continuing suffering of and devastation upon all sectors of the Indonesian peoples, in all aspects of their human, built and natural environments as inflicted by these natural hazards of earthquake, volcano and tsunami.

In the period 2000BC - 2001AD, 179 destructive tsunamis are documented to have occurred in the region. The return period for such tsunamis is difficult to explicitly determine however, a deterministic view would suggest one tsunami occurrence every 10 to 25 years. The tsunamigenic sources are either earthquakes or volcanoes or landslides (resulting from earthquakes or volcanoes). While the majority of these relate to near-field sources (within the Indonesian region), far-field sources (within the Pacific Ocean and Indian Ocean Basins) must also be considered. Because of this wide-spread nature of the tsunamigenic sources, the tsunami parameters, relative to a specific site under consideration, cover a very wide range. For near-field sources, tsunami travel times range from minutes to several hours, with wave heights and runup heights varying from less than one metre to many tens of metres. This makes tsunami warnings a very difficult matter. For far-field sources, travel times range from a few hours up to 20 hours, with wave heights and runup heights usually very small.

The central element of a tsunami hazard assessment (and thus a risk assessment) is a comprehensive tsunami data base. Such has been developed as the provisional CERA Indonesia Tsunami Data Base (CITDB), compiled from all published information available through 2001. Based on this CITDB, a preliminary analysis determined several tsunami functional relationships.

It is clear that the awareness of this natural hazard of tsunami for the Indonesian region must be understood. Tsunami mitigation strategies and measures should be taken into consideration in risk management, emergency planning procedures and engineering design of potential commercial development projects. This study was part of a project in planning for a major engineering project.

TECTONIC SETTING FOR INDONESIA

Over the last 40 years, detailed studies have provided great insight into the complex situation of the Indonesian region (for example: Hamilton, 1979; Addicott and Richards, 1986; Hall, 1996, Hamzah et al, 2000). Tectonic studies of particular areas within the Indonesian region have also been undertaken, most of which are published in the Indonesian and Japanese earth science literature.

To briefly summarise. the region has a very complicated system of plate convergences consisting of subduction, collision, back-arc thrusting and back-arc basins. This relates to the major Eurasian, Indo-Australia. Pacific, Caroline and Philippine Sea plates, and several minor plates including the Molucca Sea plate. These plates are moving relative to each other in a combination of many directions. The tectonics are identified in terms of:

(a) Three major trenches : Java, Timor, Philippines

(b) Five active island arcs:

. Sunda -convergence of Indo-Australia and Eurasian plates/ underthrusting at Java Trench
-western islands of Andaman, Sumatra and Java
-eastern islands of Bali, Lombok and Sumba

- Banda -convergence (collision) of Indo-Australian and Eurasian plates/underthrusting at Timor Trench
  - islands of Bali, Lombok, Flares and Tanimbar islands of Ceram and Bum
- Sangihe
- Halmahera
- North Sulawesi

W Major fault : Sarong Fault in western Irian Jaya I northern Banda Sea.

This complex and active tectonic situation is manifested in the very high seismic activity and significant numbers of active volcanoes.

In the global perspective of plate tectonics, the very high level of earthquake occurrence in the Indonesian region is well known (for example: Bolt, 1993; Hamzah et al, 2000). These earthquakes occur over the entire range of focal depths - shallow, intermediate, deep. In their own right, many of these earthquakes have inflicted great devastation in many areas.

Volcanoes are the other manifestation of global plate tectonics (Simkim and Siebert. 1994). They occur in those areas "behind" the trenches (or subduction zones) as a consequence of heated mantle rocks relative to the down-going slate being forced through the Earth's crust to the surface. Indonesia leads the world in both the number and the global proportion of eruptions in each of the four eruptive characteristics - fatalities, destruction of land and property, mudflows and tsunamis. The levels of these effects are closely followed by the volcanic eruptions in the Philippines. The distribution of volcanoes in this region is given in the CD ROM of Gusiakov and Hagemeyer (2000).

Although the incidence of tsunami is a well documented, common and frequently devastating natural disaster in the Indonesian region, their nature, mechanism and regional characteristics are not well known. Tsunamis are a consequence of both earthquake and volcano, and are also known to have been generated by collateral landslide occurrences.

TSUNAMIGENIC SOURCES RELATIVE TO INDONESIA

All tsunamis catalogued in this CITDB were caused by NEAR-FIELD sources, that is, within the Indonesian region. This also includes sources related to the highly seismic areas of the Philippine Trench - Southern Mindanao (Philippines). The vast majority, namely 153, were caused by earthquakes. Of the remainder, volcanic eruptions accounts for 26 tsunamis, landslides associated with earthquakes four (4) and landslides associated with volcanic eruptions one (1). Maps of such sources can be found in the CD ROM of Gusiakov and Hagemeyer (2000).

FAR-FIELD tsunamis are those generated primarily by earthquakes in the Pacific Ocean and Indian Ocean Basins. A preliminary search of the Worldwide and Pacific Ocean Basin data bases I catalogues (Gusiakov and Hagemeyer, 2000 - HTDB CDROM; NOAA-NGDC; USGS-NEIC) indicates that while several large tsunamis may(?) have been observed on tide-gauge recordings in the Indonesian Region, the wave heights (or equivalent run-ups) may be presumed to have been less than 20cm. It is noted that some of these large tsunamis were recorded on tide-gauges in the US Possessions in the Western Pacific (Caroline Is, Yap Is. Paula; Lander and Lockridge. 1969) and in eastern Australia (Rynn and Davidson, 1999). On the average, the recorded wave heights were lo-20cm, with the rare occasion of the order of Im (for example: 1960 Chile recorded in Sydney, Australia). However, a systematic search of the Indonesian records would be required to definitely determine such far-field tsunami wave heights and runups.

TSUNAMI DATA BASE FOR INDONESIA - CITDB (PROVISIONAL)

A provisional tsunami data base was compiled for the Indonesian region - CERA Indonesian Tsunami Data Base (CITDB) for the period ZOOOBC - 2001AD to include the region 9'N - 10% and 104% - 139'E.

The CITDB was compiled from all available relevant published data bases / catalogues, as listed in Table 1. The most recent data bases, the HTDB of Gusiakov and Hagemeyer (2000) and that of Hamzah et al (2000) (the latter regarded by Indonesian authorities as the most up-to-date study on the subject) were used as the "master" lists.

This CITDB, prepared as Table 2, contains the relevant information on the tsunamigenic source parameters, tsunami parameters and resulting socio-economic effects of the impacts (explanation of parameters given in Table 3). 179 tsunamis are listed.

The limitations and uncertainties in all tsunami data bases (catalogues), including this CITDB, need to be clarified. It is considered that information on and understanding of tsunami in the Indonesian region is the least known of all such areas around the globe (pers.comm., Pacific Tsunami Warning Centre. Hawaii, 2000). It is only very recently that a more intensive scientific interest is being taken, clearly because of the several devastating tsunamis that have occurred over the last decade. This relates primarily to the completeness and availability of Indonesian records and data. In the historic data record, there is always the possibility that a "tsunami" may have been caused by local flooding resulting from meteorological phenomena, particularly storm surges.

In the development of CITDB. many inconsistencies between the various data bases / catalogues for the parameters for several specific tsunamis were noted. Hence **CAUTION** must be exercised in undertaking statistical analyses of the data bases (such as the functional relationships) in the assessment of the tsunami hazard (return period, probability statements, etc).

In terms of the distress and disruption to normal life (the "socio-economic effect"). the combined forces of earthquake, volcano and landslide have taken more than 250,000 lives (and this figure relates only to those deaths reported - with the very diverse population, the true number is considered to be much greater) and have been responsible for the destruction of countless villages and towns along with their local economies. While no official estimate is available for such losses due to tsunami alone, it is clearly evident from the CITDB that a significant proportion of losses has resulted from tsunami.

TABLE 1

AVAILABLE TSUNAMI DATA BASES FOR INDONESIAN REGION

(DATA : ZOOOBC _ ZOOIAD)

Published information on tsunamis in the Indonesian Region defined within Q.OO'N to 10.00'S; 104.00'E to 140.00'E (including Indonesia (except Sumatra) and Southern Philippines).

		PUBLICATION	TSUNAMI DATA	
IATA	TYPE	REFERENCE	TIME PERIOD	REGION
002	LISTING	ITIC Tsunami Newsletter Vol XXXIV No. 1	2001 DEC	Pacific Ocean Basin
001	LISTING	ITIC Tsunami Newsletter Vol XXXIII Nos. I-5	2001 JAN - NOV 2000 DEC	Pacific Ocean Basin
1000	LISTING	ITIC Tsunami Newsletters Vol XXXII Nos.I-2	2000 JAN - NOV	Pacific Ocean Basin
:000	CATALOGUE (CDROM)	Gusiakov and Hagemeyer (2000)	2000BC 2000AD	Pacific Ocean Basin and Caribbean
1000	CATALOGUE	Hamzah et al (2000)	1600 1999	Indonesia
999	CATALOGUE	Davidson and Rynn (1998) Rynn and Davidson (1999) CERAfBoM unpublished files	1788-1995	Pacific Ocean and Indian Ocean Basins
993	CATALOGUE	Lander et al (1993)	1806-1992	Pacific Ocean Basin
992	CATALOGUE	Dunbar et al (1992)	215080 - 199IAD	Worldwide
992	CATALOGUE	Soloviev et al (1992)	1969 1982	Pacific Ocean Basin
989	CATALOGUE	Lander and Lockridge (1989) Caribbean	1690 1988	Pacific Ocean Basin
1986	CATALOGUE	Hedervari (1986)	1900-1959	Worldwide
1984	CATALOGUE	Hedervari (1984)	1500BC - 1899AD	Worldwide
1984	MAP	Lockridge and Smith (1989)	1900 - 1983	Pacific Ocean Basin
1984	CATALOGUE	Soloviev and Go (1984)	173.1968	Western Shore of Pacific OCC?I"
1977	CATALOGUE	Everingham (1977)	1768-1972	New Guinea, Solomon Is
I970	CATALOGUE	Cox (1970)	416 1969	Indonesia. Philippines China, Taiwan
1969	CATALOGUE	Pararas-Carayannis (1969)	1813.1968	Pacific Ocean Basin
1969	CATALOGUE	Berninghausen (1969)	416.1965	Indonesia. Philippines China, Taiwan
1966	CATALOGUE	Berninghausen (1966)	1750.1945	Indian Ocean and Indonesia
1947	CATALOGUE	Heck (1947)	479BC 1946AD	Worldwide

TABLE 2
CITDB : TSUNAMI DATA BASE FOR INDONESIAN REGION 2000BC - 2000AD
NEAR-FIELD TSUNAMIGENIC SOURCES
(PROVISIONAL)

DATE	TSUNAMIGENIC SOURCE							TSUNAMI PARAMETERS						SOCIO ECONOMIC EFFECTS	
	TYPE	LATITUDE	LONGITUDE	LOCATION	EARTHQUAKE FOCAL DEPTH (KM)	MAGNITUDE ML MS MW	VOLCANO	Tm	I(T)	WAVE HEIGHT MAX M	LOCALITY	RUN-UP MAX M	LOCALITY	DEATHS	DAMAGE
416 SEP 10	V	10.00°S	105.45°E	Sunda St				3.0	3.5	obs	Sunda St	(>15)	Sunda St	many	extreme
1608 JUL 1	V						Tidore				Makian Is		Makian St		limited
1629 AUG 1	E	4.30°S	129.60°E	Banda Sea		7.0		4.0	3.0	*15.0*	*Palau*	*16*	*Bandaneira*		*severe*
1659 NOV 11	V	6.90°S	129.20°E	Banda Sea			Teun			1.5	Ambon				limited
1659 DEC	E			*Ceram*									*Buru*		
1673 MAY 20	V	1.37°N	127.52°E	Halmahera			Gamkonora			mod	Ternate	mod	Ternate	many	
1673 AUG 12	E	*0.80°N*	*127.30°E*	*Halmahera*						*mod*	*Ternate*		Ternate		extreme
	V	0.80°N	127.32°E	Halmahera	(assoc. with earthquake?)		Ternate	1.0	1.0	mod	Ternate		Ternate		
1674 FEB 17	E	3.50°S	128.20°E	Ceram		8.0		6.0	4.0			100.0	Ceyt	2970	extreme
1674 MAY 06	E	3.40°S	128.00°E	Ceram		6.0		1.0		weak	Ambon				
1708 NOV 28	E	3.00°S	128.00°E	Ceram				2.0	2.0	mod	Ambon				severe
1710 MAR 06	E	4.30°S	129.60°E	Banda Sea				1.0	1.5				Bandaneira		moderate
1711 SEP 05	E	4.00°S	129.00°E	Banda Sea				1.0	1.5	1.2	Ambon		Ambon		moderate
1749 AUG 11	V	14.00°N	121.00°E	Philippines			Taal								
1754 MAY 13	V	14.00°N	121.00°E	Philippines			Taal								
1754 AUG 18	E	3.50°S	128.50°E	Banda Sea		6.5				mod	Haruku		Haruku		severe
1754 SEP 07	E	3.50°S	128.50°E	Banda Sea				1.0		mod	Haruku		Haruku		
1754 NOV 28	V	14.00°N	121.00°E	Philippines			Taal								limited
1757 AUG 24	E	6.00°S	107.00°E	Sunda St						0.5	Jakarta				
1763 SEP 01	V	0.80°N	127.32°E	Halmahera			Ternate	(0.0)		9.0	Ternate	obs	Ternate		

TABLE 2 (Continued)

DATE	TSUNAMIGENIC SOURCE									TSUNAMI PARAMETERS						SOCIO ECONOMIC EFFECTS	
	TYPE	LATITUDE	LONGITUDE	LOCATION	EARTHQUAKE FOCAL DEPTH	MAGNITUDE ML	MS	MW	VOLCANO	Tm	I(T)	WAVE HEIGHT MAX M	LOCALITY	RUN-UP MAX M	LOCALITY	DEATHS	DAMAGE
1763 SEP 12	E	4.30°S	129.60°E	Banda Sea							2.5	9.0	Bandaneira	>10.0	Bandaneira	7	extreme
1770 (?)	E	5.00°S	102.00°E	Sumatra			7.0				0.5				Bengkulu		
1775 APR 19	E	4.00°S	128.00°E	Ceram						).0)		weak	Ambon				
1802 AUG	E	4.00°S	128.00°E	Ceram						.0)			Ambon	large	Ambon		severe
1814 (?)	E	11.00°S	124.00°E	Timor						.0)					Kupang		
1815 APR 11	V	8.20°S	118.00°E	Sumbawa					Tambora	).0	1.5	3.5	Tambora	6.0	Tambora	92,000	extreme
1815 NOV 22	E-L	8.00°S	115.20°E	Bali	122		7.0			.0	1.5	large	Bali	large	Bali	10,253	extreme
1818 MAR 18	E	4.00°S	101.50°E	Sumatra			7.0				1.5			large	Bengkulu		moderate
1818 NOV 08	E	7.00°S	117.00°E	Bali	600		8.5				2.0	large	Bali St	3.5	Bali St		moderate
1820 DEC 29	E	7.00°S	119.00°E	Sumbawa	80		8.5			).0	3.5	25.0	Bulukumba	400	Nipanipa	500	extreme
1823 SEP 09	E	6.50°S	108.50°E	Java	150		8.5				-1.5			0.3	Ceribon		
1833 NOV 24	E	3.50°S	102.20°E	Sumatra	75		8.2				2.5	large			Bengkulu		moderate
1836 MAR 05	E	8.00°S	119.00°E	Sumbawa										obs	Bima		
1836 NOV 28	E	8.00°S	119.00°E	Sumbawa										obs	Bima		
1843 FEB 07	E	7.20°S	114.00°E	Java			6.0					obs	Genteng				
1845 FEB 08	E	1.30°S	124.50°E	Sulawesi			7.0					obs		large	Kema		severe
1846 JAN 25	E	2.00°N	126.50°E	Halmahera			7.2				0.5	mod	Ternate	1.2	Ternate		moderate
1851 MAY 04	E	5.00°S	105.00°E	Sumatra							1.5			1.5	Telukbetung		
1852 JAN 09	E	5.00°S	105.00°E	Sumatra										obs	Telukbetung		
1852 NOV 06	E	5.00°S	130.00°E	Banda Sea								obs	Ambon				
1852 NOV 26	E	4.30°S	129.50°E	Banda Sea	100		8.2			).0	2.5	8.0	Ambon	8.0	Bandaneira	60	extreme
1852 DEC 25	E	5.00°S	130.50°E	Banda Sea			7.0				2.0			obs	Bandaneira	few	severe
1854 JAN 04	E	3.50°S	128.60°E	Ceram			6.0							obs	Haruku		
1854 SEP 27	E	1.00°N	127.33°E	Halmahera								obs	Ternate				none
1856 MAR 02	V	3.67°N	125.50°E	Sangihe					Awu	.0	1.0	obs	Sangihe	obs	Tahuna	2806	extreme
1856 JUL 25	E	8.50°S	116.00°E	Lombok								obs	Ampenam				
1857 MAY 13	E	8.00°S	125.50°E	Timor	50		7.0			.5	2.0	3.0	Dili	(<6.0)	Likisia	40	severe
1857 NOV 17	E	1.00°N	125.00°E	Sulawesi							1.5	obs	Ternate	large	Ternate		moderate
1857 NOV 18	E	1.00°N	125.00°E	Sulawesi								obs	Kema				
1858 DEC 13	E	1.00°N	126.00°E	Sulawesi			7.4			.0	1.5	obs	Ternate	obs	Ternate		severe

TABLE 2 (Continued)

DATE	TSUNAMIGENIC SOURCE								TSUNAMI PARAMETERS						SOCIO ECONOMIC EFFECTS	
	TYPE	LATITUDE	LONGITUDE	LOCATION	EARTHQUAKE FOCAL DEPTH	MAGNITUDE ML	MS	MW	VOLCANO	Tm	I(T)	WAVE HEIGHT MAX M	LOCALITY	RUN-UP MAX M	LOCALITY	DEATHS	DAMAGE
1859 JUN 28	E	1.00°N	126.50°E	Halmahera			7.0			3.0	3.0	obs	Ternate	10.0	Sidangoli		limited
1859 JUL 20	E	5.00°S	130.00°E	Banda Sea								obs	Lonthor				
1859 JUL 29	E	0.00°N	125.50°E	Sulawesi			7.2			1.0	1.5	mod	Kema	obs	Bangai		moderate
1859 SEP 25	E	5.50°S	130.50°E	Banda Sea			6.7			1.0	0.5	obs	Bandaneira	obs	Bandaneira		
1859 OCT 20	E	9.00°S	111.00°E	Java							1.0	obs	Patjatan	mod	Patjatan		limited
1859 DEC 17	E	2.00°N	125.00°E	Sulawesi										obs	Belang		
1859 DEC 26	E	2.00°N	125.00°E	Sulawesi						1.0				obs	Kema		limited
1860 OCT 06	E	1.40°S	128.50°E	Halmahera								obs					
1861 JUN 05	E	6.30°S	107.30°E	Java						1.0					Karawang		
1864 MAY 23	E	1.00°S	135.00°E	Irian Jaya			7.8			1.5	1.5	3.0	Geelvink	12.0	Geelvink	250	
1871 MAR 02	V	2.27°N	125.42°E	Sangihe					Ruang	4.0	3.5	large	Tahulandang	25.0	Buhias	460	extreme
1875 MAR 28	E	8.30°S	110.70°E	Java										obs	Sth Java		
1865 MAY 28	E	3.00°S	127.20°E	Ceram			6.8					obs	Buru	0.3	Kayali		limited
1882 OCT 10	E	5.00°S	130.00°E	Banda Sea								obs	Bandaneira				
1883 AUG 26	V	6.10°S	105.40°E	Java					Krakatau								
1883 AUG 27	V	6.10°S	105.40°E	Java					Krakatau		4.5	large	Sunda St	35	Merak	00,000	catastrophic
1884 JAN	V	6.10°S	105.40°E	Java					Krakatau			obs					
1885 APR 30	E	2.50°S	128.50°E	Ceram			7.2				0.5	obs	Kayeli	1.2	Djikomurasa		severe
1889 SEP 06	E	1.00°N	125.60°E	Sulawesi	70		8.0			1.0	2.5	9.0	Bentenan	4	Kema		severe
1889 SEP 09	V	3.14°N	125.49°E	Sangihe					Banau Wuhu			1.5	Tareona				
1889 NOV 23	E	7.00°S	113.50°E	Java			6.0				1.0	obs	Madura				
1891 OCT 05	E	9.00°S	124.00°E	Sunda St	80		7.0				0.5	obs	Ende	obs	Ende		
1892 JUN 07	V-L	3.67°N	125.50°E	Sangihe					Awu	1.0	1.0	1.5	Ambon			1,532	severe
1892 NOV 18	E	3.00°S	127.80°E	Ceram	70		7.0				-1.0	obs	Kayeli				
1896 APR 18	E	8.00°S	125.00°E	Timor										obs	Alor	250	
1896 OCT 10	E	3.50°S	102.50°E	Sumatra	130		6.8					obs	Singkel				
1897 JAN 03	E	6.00°N	122.70°E	Philippines			8.2							obs	Sulu	100	
1897 MAR 15	E	6.80°S	120.80°E	Flores	15		5.5				1.0	obs	Kajuadi				
1897 SEP 21	E	6.80°N	122.00°E	Philippines			8.6				1.0	obs	Jolo				
1897 SEP 21	E		122.10°E	Philippines						1.0	2.5	6.0	Jolo	7.0	Isabela	100	severe

TABLE 2 (Continue

DATE	TSUNAMIGENIC SOURCE								TSUNAMI PARAMETERS						SOCIO ECONOMIC EFFECTS	
	TYPE	LATITUDE	LONGITUDE	LOCATION	EARTHQUAKE FOCAL DEPTH	MAGNITUDE ML	MS	MW	VOLCANO	n	I(T)	WAVE HEIGHT MAX M	LOCALITY	RUN-UP MAX M	LOCALITY	DEATHS	DAMAGE
1899 SEP 29	E-L	3.50°S	128.50°E	Banda Sea	60		7.8			0	3.0	9.0	Ceram	12.0	Tehorw	3,864	extreme
1900 JAN 10	E			Halmahera								obs	Galela				
1900 OCT 08	E	3.50°S	136.00°E	Irian Jaya	33		7.8				1.5	obs		(<6.0)	Napan	5	limited
1902 AUG 21	E	6.30°N	123.60°E	Philippines			7.2							obs	Iliana	many	severe
1903 MAR 30	E	3.00°S	127.50°E	Ceram			6.5					1.0	Tifu	(<2.0)			
1907 MAR 30	E	3.00°N	122.00°E	Celebes Sea	500		7.3				1.5	obs	Talaud	4.0	Karakelong	400	extreme
1908 MAR 24	E	8.70°S	124.70°E	Timor			6.6			0				25.0	Atupupu		
1910 DEC 18	E	4.00°N	127.00°E	Talaud	33		6.7				-1.0	obs	Lirung	(<2.0)			
1913 MAR 14	E	4.80°N	126.60°E	Sangihe	25		8.3							obs			
1914 MAY 26	E	2.00°S	137.00°E	Irian Jaya	60		7.9	7.9		0	2.0			<6.0	Pom	many	moderate
1915 NOV 06	E	1.00°S	136.00°E	Irian Jaya			6.0							obs	Korim		
1917 JAN 21	E	8.00°S	115.40°E	Bali	33		6.5							obs	Bali	15,000	severe
1917 JAN 31	E	5.60°N	124.80°E	Philippines	33		6.4					1.5	Glan	<2.0		7	limited
1918 JUL 18	V	3.14°N	125.49°E	Sangihe					Banua Wuhu								
1918 AUG 15	E	5.77°N	123.64°E	Philippines	57		8.3	8.2		5	2.5	obs	Halmahera	7.0	Glan	102	severe
1919 JAN 01	E	7.28°N	126.88°E	Philipines	9		7.4	7.0		.0							
1920 JAN 29	*E*	*0.00°N*	*124.00°E*	*Sulawesi*								obs	Gorontalo	*2.0*	*Donggala*		
1921 MAY 14	E	0.70°N	117.90°E	Kalimantan	20		6.2				0.5			1.0	Sekurau		moderate
1921 SEP 11	E	11.00°S	111.00°E	Java			7.5					0.1	Tjilatjap				
1921 SEP 29	E	8.00°N	127.00°E	Philippines	10		7.5				0.5			1.9			
1921 NOV 11	*E*	*8.00°N*	*127.00°E*	*Philippines*	*60*		*7.5*	*7.3*			*1.0*	*obs*	*Sangihe*	*(<2.0)*	*Manay*	*600*	*moderate*
1922 SEP 01	E	9.00°N	123.30°E	Philippines	33		6.0				0.5	obs	Negros	0.1	Zamboanga		limited
1923 FEB 23	E	6.75°N	123.56°E	Philippines							0.5	obs	Cotabato				
1923 MAR 02	E	7.63°N	124.85°E	Philippines	94		7.2	7				obs	Cotabato	(<2.0)			
1923 JUL 18	*E*	*9.50°N*	*125.00°E*	*Philippines*	*33*		*5.5*				*1.0*	*large*	*Mambajao*	*(<2.0)*	*Mambajao*		*limited*
1924 APR 14	E	6.79°N	126.08°E	Philippines	14		8.3	8.1			0.5	large	Caraga	(<2.0)	Binuangan		moderate
1924 AUG 30	E	9.04°N	126.18°E	Philippines	115		7.2	7.1			0.5	obs	Bislig	(<2.0)			moderate
1925 JAN 08	E	8.00°S	116.00°E	Bali								obs	Butung	(<2.0)			
1925 MAY 05	*E*	*9.72°N*	*123.02°E*	*Philippines*	*16*		*6.8*				*0.5*			*(<2.0)*	*Negros*	*17*	*moderate*
1927 AUG 07	V	8.32°S	121.71°E	Flores					Paluweh	0	3.0	10.0	Palu	10.0	Palu	226	severe

TABLE 2 (Continued)

DATE	TSUNAMIGENIC SOURCE								TSUNAMI PARAMETERS						SOCIO ECONOMIC EFFECTS	
	TYPE	LATITUDE	LONGITUDE	LOCATION	EARTHQUAKE FOCAL DEPTH	MAGNITUDE ML	MS	MW	VOLCANO	Tm	I(T)	WAVE HEIGHT MAX M	LOCALITY	RUN-UP MAX M	LOCALITY	DEATHS	DAMAGE
1927 DEC 01	E	0.50°S	119.50°E	Sulawesi	33		6.0			.0	3.0	obs	Palu	15.0	Palu	14	severe
1928 MAR 26	V	6.10°S	105.40°E	Java					Krakatau			obs					
1928 DEC 19	E	6.87°N	124.84°E	Philippines	12		7.3	7.3				obs	Illana	(<2.0)	Cotabato	4	moderate
1929 JUN 13	E	7.95°N	126.76°E	Philippines	51		7.2	7.0				obs	Hinatuan	(<2.0)			moderate
1930 MAR 17	V	6.10°S	105.40°E	Java					Krakatau			500	Krakatau				
1930 JUN 19	E	5.60°S	105.30°E	Java	33		6.0					obs	Telukbetung	(<2.0)			
1930 JUL 19	E	9.30°S	114.30°E	Bali	33		6.5					0.1	Besuki	(<2.0)			
1930 SEP 11	E	2.00°N	124.00°E	Sulawesi										(<2.0)	Amurang		
1931 SEP 25	E	5.41°S	102.34°E	Sumatra	87		7.5	7.3						1.0	Enggano		limited
1932 SEP 09	E	3.60°S	128.30°E	Ceram	33		8.2					obs	Piru	(<2.0)			moderate
1934 JUL 19	E	0.73°S	133.36°E	Irian Jaya	15		7.0					obs					
1936 APR 01	E	4.18°N	126.55°E	Talaud	54		7.7	7.6			1.5	obs	Sangir	3.0	Salebabu		severe
1937 NOV 06	E	3.00°S	132.00°E	Irian Jaya			6.0							(<2.0)			
1938 FEB 02	E	5.10°S	131.53°E	Banda Sea	30		8.2	8.2		.5		1.0	Tual	(<6.0)	Tajandu		severe
1938 FEB 13	E	3.00°S	132.00°E	Irian Jaya								0.5	Fakfak	(<2.0)			
1938 MAY 19	E	1.00°S	120.00°E	Sulawesi	60		7.9			.5		3.0	Tomini	3.0	Toribulu	16	severe
1938 OCT 10	E	2.41°N	126.67°E	Halmahera	70		7.3	7.1			-2.0			0.1			
1939 DEC 21	E	0.01°N	122.68°E	Sulawesi	150		8.6					obs	Tomini	(<2.0)	Langoan		extreme
1950 OCT 08	E	3.80°S	128.30°E	Banda Sea	60		7.6	7.4			1.5			(<6.0)			
1952 MAR 19	E	9.50°N	127.20°E	Philippines	25		7.9	7.6			-2.0	0.7	Palau				
1957 JUN 22	E	1.94°S	136.62°E	Irian Jaya	35		7.3	7.3		.0				1.8			
1957 SEP 26	E	8.20°S	107.30°E	Java	33		5.5							(<2.0)			
1957 OCT 26	E	2.00°S	116.00°E	Kalimantan	33		6.0							(<2.0)			
1958 APR 21	E	4.58°S	104.09°E	Sumatra	179		6.5					obs		(<2.0)			
1963 DEC 16	E	6.50°S	105.38°E	Java	53		6.5					obs	Labuhan	(<2.0)			
1965 JAN 24	E	2.46°S	125.96°E	Ceram	30		7.6	8.0		.0	1.5	obs	Sanana	(<6.0)	Sanana	71	severe
1967 APR 11	E	3.47°S	119.07°E	Sulawesi	19		5.8				1.5	obs	Tinambung	(<6.0)	Tinambung	58	severe
1968 AUG 10	E	1.42°N	126.26°E	Sulawesi	19		7.6	7.5		.0	-2.0	obs		0.14			
1968 AUG 14	E	0.06°N	119.70°E	Sulawesi	17		7.7	7.3		.0	3.0	10.0	Donggala	10.0	Donggala	392	severe
1969 FEB 23	E	3.18°S	118.80°E	Sulawesi	60		6.9			.0	1.5	4.0	Paletoang	(<6.0)	Madjene	600	severe

TABLE 2 (Continued)

DATE	TSUNAMIGENIC SOURCE								TSUNAMI PARAMETERS						SOCIO ECONOMIC EFFECTS	
	TYPE	LATITUDE	LONGITUDE	LOCATION	EARTHQUAKE FOCAL DEPTH (KM)	MAGNITUDE ML	MS	MW	VOLCANO	Tm	I(T)	WAVE HEIGHT MAX M	LOCALITY	RUN-UP MAX M	LOCALITY	DEATHS	DAMAGE
1970 JAN 10	E	6.79°N	126.68°E	Philippines	60		7.3				-3.0	0.1	Davao				
1972 DEC 02	E	6.47°N	126.65°E	Philippines	80		7.8	8.0		-1.0	-1.0	0.5		<2.0			moderate
1975 JAN 15	E	5.00°S	130.00°E	Banda Sea			5.9					obs	Bandaneira				limited
1975 MAR 05	E	2.40°S	126.10°E	Sulawesi			6.5			1.0				1.2	Sanana		limited
1976 AUG 16	E	6.28°N	124.08°E	Philippines	58		8.0	8.1		-1.0	2.5	4.8	Moro	5.0	Alicia	8000	extreme
1977 AUG 19	E	11.13°S	118.38°E	Sumba	21		8.0	8.3		3.0	3.5	30.0	Sumba	15.0	Sumba	189	severe
1978 JUN 14	E	8.28°N	122.40°E	Philippines	36		6.9			0.0		obs		<2.0			
1979 APR 15	E	3.11°N	128.15°E	Halmahera	125		5.0			0.0							
1979 JUL 18	E-L	8.50°S	123.50°E	Flores						3.0	3.0	9.0	Lomblen	10.0	Lomblen	539	severe
1979 SEP 12	E	1.69°S	135.97°E	Irian Jaya	21		8.1	7.5			0.0	obs	Biak	2.0	Yapan	100	severe
1982 DEC 25	E-L	8.40°S	123.00°E	Flores	33		5.9			(1.0)				obs	Larantuka	13	moderate
1983 MAR 12	E	4.09°S	127.85°E	Banda Sea	30		6.0	6.1			1.5			3.0	Ambon		
1984 JAN 08	E	2.90°S	118.70°E	Sulawesi	43		6.6					obs	Mamoju				
1985 APR 13	E	9.21°S	114.20°E	Bali	88		6.2	5.9									
1987 NOV 26	E	8.40°S	124.30°E	Flores	33		6.2			1.0				obs	Pantar		
1989 JUL 14	E	8.10°S	125.10°E	Flores	52		6.2			0.0				obs	Alor	7	limited
1989 JUL 31	E	8.10°S	121.40°E	Flores			6.3			0.0				obs	Maumere	3	limited
1990 APR 18	E	1.20°N	122.82°E	Sulawesi	36		7.4	7.6									
1992 MAY 17	E	7.23°N	126.75°E	Philippines	63		7.5	7.2									
1992 JUN 20	E	1.96°N	122.80°E	Sulawesi			6.2			0.0				obs	Kuandang		
1992 JUL 04	E	8.10°S	124.70°E	Flores			6.2					obs	Alor	obs	Kalabahi	23	moderate
1992 DEC 12	E	8.50°S	121.84°E	Flores	29		7.5	7.7			2.7	25.0	Maumere	26.18	Maumere	2200	extreme
1994 JAN 21	E	1.04°N	127.77°E	Halmaherea	19		7.3	6.9			1.5			2.0	Maluku		
1994 FEB 15	E	5.01°N	104.26°E	Sumatra	23		7.0	6.8									
1994 JUN 02	E	10.42°S	112.91°E	East Java	34		7.2	7.8			2.5			13.9	Sumba	250	severe
1994 OCT 08	E	1.21°S	127.98°E	Halmahera	17		6.8	6.8			1.5			3.90	Obi	1	moderate
1995 JAN 27	E	4.46°S	134.45°E	Irian Jaya	26		6.8	6.8									
1995 FEB 13	E	1.33°S	127.48°E	Halmahera	19		6.8	6.7			1.5			3.0	Obi	1	moderate
1995 MAR 19	E	4.14°S	135.11°E	Irian Jaya	28		7.1	6.8									
1995 MAY 14	E	8.47°S	125.04°E	Timor	20		7.0	6.9			1.5			4.0	E. Timor	8	limited

TABLE 2 (Continued)

DATE	TSUNAMIGENIC SOURCE								TSUNAMI PARAMETERS				SOCIO ECONOMIC EFFECTS	
	TYPE	LATITUDE	LONGITUDE	LOCATION	EARTHQUAKE FOCAL DEPTH (KM)	MAGNITUDE ML	MS	MW	VOLCANO	Tm I(T)	WAVE HEIGHT MAX M	LOCALITY	RUN-UP MAX M	LOCALITY	DEATHS	DAMAGE
1996 JAN 01	E	0.70°N	119.90°E	Sulawesi	25		7.7	7.9		1.8			3.43	Palu	24	Severe
1996 FEB 17	E	0.92°S	136.98°E	Irian Jaya	35		8.1	8.2		1.8			7.68	Biak	108	Severe
1998 NOV 29	E	1.97°S	124.88°E	Sulawesi	22		7.6	7.7		1.5			2.75	Taliabu	34	moderate
2000 MAY 04	*E*	*1.11°S*	*123.57°E*	*Sulawesi*	*26*		*7.5*	*7.6*		*1.0*			*5.00*			
2000 JUN 04	E	4.72°S	102.09°E	Sumatra	33		8.0	7.9								

TABLE 3

CITDB : TSUNAMI DATA BASE FOR INDONESIAN REGION 2000BC - 2001AD
(PROVISIONAL)

EXPLANATION OF PARAMETERS

DATE: All dates are in Universal Coordination Time UT

TSUNAMIGENIC SOURCE

TYPE: E Earthquake
V Volcano
E-L Landslide caused by earthquake
V-L Landslide caused by volcano

EARTHQUAKE PARAMETERS : Where applicable, these parameters referred To the USGS-NEIC earthquake catalogues and US-NOAA tsunami catalogues.

TSUNAMI PARAMETERS

Tm Tsunami magnitude (Section 3.22; lida et al, 1967)
(. .) denotes estimated (not calculated) value

I(T) Tsunami intensity (Section 3.2.2; Goloviev and Go, 1974)

WAVE HEIGHT: Maximum value and its locality as reported
obs tsunami waves observed, no value reported
weak small tsunami waves observed, no value reported
mod significant tsunami waves observed, no value reported
large large tsunami wave observed, no value reported

RUN-UP : Maximum value and its locality reported
(.. .) denotes estimated (not calculated) value
obs runup observed, no value reported
mod significant runup observed, no value reported
large large runup observed, no value reported

SOCIO-ECONOMIC EFFECTS

DEATHS : Number of fatalities as reported noting this value is the total
Number including the original source (earthquake, volcano) and the
few small number (probably less than IO), no value reported
many large number (probably more than 50), no value reported

DAMAGE : As defined by US-NOAA including the built, natural and human Environments

limited	slight, minor, light
moderate	significant
severe	major, heavy
extreme	devastating
catastrophic	total destruction

(More detailed information can be sourced from the data bases/ catalogues referenced in TABLE 1).

TSUNAMI HAZARD ASSESSMENT (PRELIMINARY)

The information contained in the tsunami data base CITDB of TABLE 2, that is, historical tsunami data, provides an empirical method for the preliminary tsunami hazard assessment of the Indonesian region. The following elements were considered in this assessment:

1. TSUNAMI DATA BASE CITDB (TABLE 2)

The tsunami data base CITDB for the time period 2000BC 2001AD clearly shows that a significant number, 179, have impacted upon the region. Of these, 43 tsunamis have been characterised as severe/extreme, with run-up values grater than about 5m and damaging effects recorded. This historical records shows that wave heights of up to IO-20m and runup heights of up to 25m have been recorded. Such events have occurred throughout the Indonesian region, including the Indonesian Arc islands, around the Molucca Sea the near islands of Halmahera, Ceram, Talaud and Sulawesi, and in the Southern Philippines area. Note should be taken of the extreme events such as the 1883 Krakatau volcanic eruption and the 1874 Ceram and 1820 Sumbawa earthquakes where reports suggest runup heights of hundreds of metres.

2. TSUNAMI PARAMETERS

The complete set of tsunami parameters should include those parameters relating to both the "source" of the tsunami generation and the "effects" at the point of maximum tsunami impact.

(a) Tsunamigenic source parameters:

earthquake	origin time, epicentre, focal depth, moment magnitude MW, focal mechanism
volcano	name, location coordinates, type of disruption volcano eruption index (per Acharyn, 1989)
landslide -	cause, origin time, location, type/description

(b) Tsunami effects parameters (at impact site):

wave height -	actual height of tsunami waves in open water; instrumentally recorded on tide-gauges with wave parameters taken from marigrams; anecdotal information (observer location, description of waves, estimated wave heights)
runup	maximum vertical height on land that tsunami waves have reached, above a reference sea level

CAUTION: Questions have been raised as to the validity of some runup values published in tsunami data bases/catalogues. It is has been shown that in some cases such "runup" values were actually wave heights. This issue must be taken into consideration when using published "runup" values for the derivation of other tsunami parameters.

Tide state	In considering the potential effects of tsunami impacts on Coastlines in terms of runup values, the state of the tide when the tsunami reaches the shore may be critical. The maximum runup for a given tsunamic wave height will be greater at the time of high tide than at low tide. This will be accentuated in those regions which have very large ocean tide fluctuations. There is also the case where a small tsunami occurring at high tide may reach a higher elevation on shore than that for a larger tsunami occurring at low tide.

(c) derived parameters

Tm tsunami magnitude
Tm = log,H. H = runup (m) (lida et al, 1967)
I(T) tsunami intensity
I(T) = log2 (2"' H) (Soloviev and Go, 1974)

3. FUNCTIONAL RELATIONSHIPS

These analyses are based on the statistical processing of historical tsunami runup observations (per tsunami data baseslcatalogues) at particular sites. They usually refer to an area or region, rather than being site-specific. **EXTREME CAUTION** must be exercised in attempting to interpret the results for practical applications. This particularly relates to the limitations and uncertainties of the tsunami data base, specifically in terms of the quantity (usually small numbers of observations) and quality of the runup values. As this is a developing scientific tool, such results should be considered only as a guide.

For some areas, because of the sparsity of the tsunami data (that is, irregular and infrequent occurrences), consideration should be given to a deterministic approach and not just the probabilistic (statistical) methods (for example: for Australia; Rynn and Davidson, 1999).

A preliminary estimate of three hrnctional relationships using the tsunami data base and statistical relations of Gusiakov and Hagemeyer (2000) - HTDB CDROM were made for the Indonesian region in toto (taken as lOaN 10%. IIOOE - 140'E) and for a particular localised area around Halmahera Island (taken as 6'N 5% 123OE - 136OE) for a 400 year period (1600 - 2000; default status) for each case. Again, **CAUTION** must be exercised in assigning some reliability to the results.

Indonesian Region (lOoN - IO'S, IIO'E - 140°E)

Tsunami Runup Heights versus Time : A simple geographical description of the nature of tsunami occurrences in a related area. It was clearly evident that there is a probable bias in the available data from about 1800 to 1930 (times of historical exploration) and 1995 to 2000 (instrumental records available). Only 39 events were used in the analysis. A simple view may consider that since 1800, the return period for a significant tsunami event was about 10 years.

Tsunami Runup Frequency Function (F-function) : When statistical analysis that provides an empirical frequency of recurrence (that is, the reverse value to the return period) for potential runup heights.

For example: For Runup H = 20m, Return Period – 100 years
For Runup H = lOm, Return Period – 25 years.

Tsunami Hazard Function (H-function) : A statistical analysis that provides tsunami hazard curves (probability functions) showing the probability of exceedence of any selected runup height for a given period of time (the Return Period).

For example: For Runup H = 60m, Return Period T = 10 years Probability 0.01
Return Period T = 50 years Probability 0.05
Return Period T = 100 years Probability 0.10
Return Period T = 1000 years Probability 0.65.

Halmahera Island Area (6'N 5'S, 123OE - 136'E)

Tsunami Runup Heights versus Time : The same qualifications as for the Indonesian region apply. Only 17 events were used in the analysis. The return period for a significant tsunami event is even less definitive.

F function : This relationship shows, for example, that for
runup H = 20m, Return Period – 300 years
runup H = lOm, Return Period – 80 years.

H -function : While calculations were performed, no reliability can be assigned to this graph.

An example of these estimates of tsunami parameters for the localised area of Halmahera Island is given in the Table 4, where the NEAR-FIELD : LOCAL is defined as the area within 500km of Halmahera Island and NEAR FIELD : REGIONAL as the remainder of the Indonesian Region.

TABLE 4

ESTIMATES OF TSUNAMI PARAMETERS IN RELATION TO POTENTIAL TSUNAMIGENIC SOURCES FOR THE HALMAHERA ISLAND AREA

TSUNAMIGENIC SOURCE			TSUNAMI PARAMETERS RETURN PERIOD (YEARS)	WAVE HEIGHT (MAX M)	RUNUP HEIGHT (MAX M)
EARTHQUAKE	NEAR-FIELD :	LOCAL	10	>10.0	50.0
	:	REGIONAL	1-5	10.0	20.0
	FAR-FIELD :	Philippines	10	10.0	25.0
	:	Pacific Ocean	10	0.5	0.5
	:	Indian Ocean	100	(small)	(small)
VOLCANO	NEAR-FIELD :	LOCAL	25	25.0	25.0
	:	REGIONAL	100	10.0	10.0
	FAR-FIELD :	Philippines	?	(10.0?)	(10.0?)
	:	Pacific Ocean	(100?)	(small)	(small)
LANDSLIDE	NEAR-FIELD :	LOCAL			
	:	Earthquake	?	(10.0?)	(10.0?)
	:	Volcano	?	(10.0?)	(10.0?)
	:	REGIONAL			
	:	Earthquake	(100?)	10.0	10.0
		Volcano	(100?)	10.0	10.0
	FAR-FIELD :	(E-L/V-L)	?	(small)	(small)
DIAPIRS			(no information available)		
ASTEROID IMPACT			(no information available)		
NUCLEAR EXPLOSION			(no information available)		

4. POTENTIAL TSUNAMIGENIC SOURCES

The potential tsunamigenic sources considered in this hazard assessment, for both the near-field and far-field, included:

- earthquake — Indonesian Region (Gusiakov and Hagemeyer, 2000; Hamzah et al, 2000)
  Pacific Ocean and Indian Ocean Basins (Rynn and Davidson, 1999)
- volcano — Indonesian Region (Latter, 1981; Gusiakov and Hagemeyer, 2000)
- submarine landslide - turbidity currents (Tappin et al..1999; Prasad et al, 2000)
  gravity slides (Campbell and Nottingham, 1999)
  - meteorological phenomena (large storms)
- asteroid impacts (Solem, 1999)
- diapiric eruptions (DeLange and Hull, 1994)
- nuclear explosions (at sea).

Those identified in all available seismological analyses are listed in Table 5.

TABLE 5

POTENTIAL TSUNAMIGENIC SOURCES IN THE INDONESIAN REGION

EARTHQUAKE ZONES			
Southwest Sumatra, Java, Sumbawa, Sumba. Flares, Banda Sea, Sulawesi. Irian Jaya, Ceram, Sula, Sangihe, Talaud, Molucca, Halmahera. Southern Philippines			
VOLCANO			
Krakatau	Sunda Strait	6.1 O'N	105.42"E
Tambora	Sumbawa	8.25'N	118.80°E
Rokatenda	Flores	8.60°N	121.70"E
Paluweh	Flares	8.32ON	121.71'E
Yersey	Banda Sea	7.53'N	123.95"E
Emperor of China	Banda Sea	6.62ON	124.22"E
Nieuwerkerk	Banda Sea	6.60"N	124.68"E
Teen	Banda Sea	6.92"N	129.13"E
Banda Api	Banda Sea	4.52'N	129.87'E
Ternate (Gamalama)	Halmahera	0.80°N	127.33OE
Gamkonora	Halmahera	1.38ON	127.52OE
Ruang	Sangihe	2.28ON	125.43OE
Banau Wuhu	Sangihe	3.67ON	125.50"E
Jolo (Bau Dajo)	Phjlippines	5.95'N	121.07'E
Taal	Philippines	14.00°N	120.99"E
LANDSLIDE			
Volcano induced	Sangihe. Ceram		
Earthquake induced	Flares, Bali		

5. SEICHE

Seiches are wave activity related to tsunamis, both being gravity waves. Whereas a tsunami is a travelling wave, a seiche is a standing wave. Seiches occur in fully or partially enclosed bodies of water such as lakes or embayments/harbours, respectively. When the period of the tsunami source wave is close to that of the normal mode of the body of water, seiches can resonate and amplitudes then increase. The potential for seiche occurrence would be in site-specific locations.

6. TSUNAMI TRAVEL TIME CHARTS

Tsunami travel times are dependent on the distance and path from source to point of impact. Account must be taken of geography of the region (shape of coastline, islands etc) for reflections and refractions of the tsunami waves. This element is vital in notification of WARNINGS and emergency procedures. At present, these are published for the Pacific Ocean Basin by the US/NOAA Pacific Tsunami Warning Centre (PTWC) in Hawaii, and for the Indian Ocean basin in the publication of Otto and Murty (1996).

7. COMPUTER MODELLING

In recent years, with the availability of more accurate bathymetric data, numerical modelling by computer has advanced to provide greatly improved theoretical estimates of tsunami wave travel times, wave heights and runup heights. Currently, extensive research is being undertaken to better delineate source characteristics, particularly gravity induced (slope) and submarine landslides.

TSUNAMI HAZARD ZONING

This preliminary tsunami hazard assessment was quantified in terms of "Tsunami Hazard Zones", a given in Table 6.

TABLE 6

TSUNAMI HAZARD ZONES (PROVISIONAL)
FOR INDONESIAN REGION

CHARACTERISTIC	TSUNAMI HAZARD ZONES		
	HI	MED	LO
RUN-UP HEIGHT	>4	24m	c2m
TSUNAMI MAGNITUDE	>2	1	<o
TSUNAMI WAVE HEIGHT	>Im	O.l-lm	<O.lm
DAMAGE OBSERVED FROM HISTORIC TSUNAMIS	SIGNIFICANT	MINOR	NONE
COASTLINE ADJACENT TO NEAR-FIELD TSUNAMIGENIC SOURCES	YES	YES	NO
POTENTIAL TSUNAMI INUNDATION IN THE FUTURE	PROBABLE	POSSIBLE	UNLIKELY

TSUNAMI VULNERABILITY ASSESSMENT

The potential damage from a tsunami impact at a site is relative to the runup height at that site. Such damage refers to the built, natural and human environments (at the coastline), and so includes coastal towns and villages, development and major industrial projects. A vulnerability assessment at a specific location can be characterised by integrating the vulnerability inventory (catalogue of attributes with comparison maps and GIS surveys) with damage assessments (if available, based on historic records of damage). This would involve both the terrestrial and marine environments, to include:

- human toll
  - deaths
  - injuries
  - socio-economic effects
- built environment
  - property
  - infrastructure
  - agriculture
- natural environment
  - topography
  - bathymetry

TSUNAMI RISK ASSESSMENT

A comprehensive risk assessment involves the integration of the hazard and vulnerability assessments, both quantitatively and qualitatively (for example: Rynn and Davidson, 1999, for Australia and its Island Territories; Prasad et al, 2000, for the City of Suva, Fiji).

TSUNAMI WARNINGS

The concept of tsunami warnings relate to emergency procedures to be taken to reduce potential losses from an impending tsunami. At this time, there appears to be no warning system in relation by Indonesia. However, normal operations of the Pacific Tsunami Warning Center in Hawaii do include Indonesia in their warnings for tsunamis generated in the Pacific Ocean Basin. There are no warnings issued for Indian Ocean Basin tsunamis.

In the event of the tsunami warning being issued, the most reliable information available is by reference to the tsunami travel time charts. However, in localised in areas of near-field tsunamis, where travel times would be less than 1-2 hours, such warnings would be far too short to enact emergency procedures (as was the case, for example, in the July 1998 Aitape, Papua New Guinea tsunami wherein travel times were about 10 minutes; Tappin et al, 1999). A provisional tsunami warning approach is given in Table 7.

TABLE 7

TSUNAMI WARNINGS (PROVISIONAL)
FOR INDONESIAN REGION

TSUNAMI CLASSIFICATION	DISTANCE (KM)	TSUNAMI TRAVEL TIME (HOURS)	TSUNAMI WARNING
NEAR-FIELD	0 - 50	< 0.5	NONE
	50 500	< 0.2	NONE
	500 - 1500	2 - 3	LIMITED
	1500 - 2500	3 - 6	PROBABLE
FAR-FIELD	>2500	6 - 16	AMPLE

SUMMARY

Tsunamis, in addition to earthquakes and volcanic eruptions, are a major natural hazard for Indonesia. Their effects have been, and have future potential to be, devastating on the coastal areas of many, if not all, of the Indonesian islands. In the historical record, the human toll, damage to the built (major centres of population, villages, buildings, infrastructure, etc) and natural environments, and disruption to the socio-economic fabric of the nation and its peoples, are well documented. The tsunamigenic sources have all been in the near-field (within the Indonesian region) as a consequence of earthquakes, volcanoes and collateral landslides.

Based on the tsunami data base CITDB, and in view of the continuous tectonic activity in the region, there is unquestionably a real and significant probability that impacts of near-field tsunamis, with consequential potential damage, will be a realistic situation in the future. Serious consideration should be given to mitigation strategies and measures for this natural hazard of tsunami in terms of both expanded hazard assessments (more detailed deterministic and probabilistic analyses of the available data and computer modelling) and vulnerability assessments. Practical applications of the consequent tsunami risk assessments would then provide a proactive approach to:

- reduction of community vulnerability
- establishment of a local tsunami warning system
- development of disaster plans
- development of evacuation plans
- risk management procedures
- implementation into engineering design of major developmental projects, both on land and in the adjacent sea areas.

ACKNOWLEDGEMENT

This study was a part of the planning stage in the engineering design (risk management procedures for natural hazards) of a major commercial development project. Access to the HTDB CDROM was kindly provided by the Commonwealth of Australia Bureau of Meteorology Queensland Regional Office, per Mr J Davidson (Regional Director). The assistance of Mr T Boen (Jakarta, Indonesia) and Dr L Hamzah (Japan) in providing Indonesian information is gratefully acknowledged.

REFERENCES

Acharya, H., 1989 : Estimation of Tsunami Hazard from Volcanic Activity Suggested Methodology with Augustine Volcano, Alaska as an Example. Natural Hazards, 1, 3410348.

Additcott, W.O. and Richards, W. (Compilers), 1986 : Plate Tectonic Map of the Circum-Pacific Ocean Southeast Quadrant. Scale 1:10,000,000. Circum-Pacific Council for Energy and Mineral Resources.

Berninghausen, W.H., 1966 : Tsunamis and Seismic Seiches Reported from regions Adjacent to the Indian Ocean. Bulletin of the Seismological Society of America, 56. 1, 69-74.

Berninghausen, W.H., 1969 : Tsunamis and Seismic Seiches of Southeast Asia. Bulletin of the Seismological Society of America, 59, 1, 289-297.

Bolt, B.A., 1993 : "Earthquakes". W.H. Freeman and Company, New York, 331pp

Campbell, B.A. and Nottingham, D., 1999: : Anatomy of a Landslide - Created Tsunami at Skagway, Alaska, November, 3, 1994. Science of Tsunami Hazards, 17. 1. 19-43.

Cox, D.C., 1970 : Discussion of "Tsunamis and Seismic Seiches of Southeast Asia" by William H. Berninghausen. Bulletin of the Seismological Society of America, 60, 1, 281-287.

Davidson, J. and Rynn, J. 1998 Summary Report for Emergency Management Australia Australian IDNDR Coordination Committee Report 1 I/94 "Contemporary Assessment of Tsunami Risk and Implications of Early Warnings for Australia and Its Island Territories, June 1998,25pp.

DeLange, W.P. and Hull, A.G., 1994 : Tsunami Hazard for the Auckland Region. Auckland Regional Council Environment Division Technical Publication No. 50, November 1994, 37PP.

Dunbar, P.K., Lockridge, P.A. and Whiteside, L.S., 1992 : Catalogue of Significant Earthquakes 2150BC1991AD. US Department of Commerce, NOAA, National Geophysical Data Center, Boulder, USA, World Data Center A for Solid Earth Geophysics Reports SE-49, 320~~.

Everingham, I.B., 1977: Preliminary Catalogue of Tsunamis for the New Guinea I Solomon Island Region 1768-1972. Bureau of Mineral Resources, Canberra, Australia, Report 180, 78pp.

Gusiakov, V.K. and Hagemeyer. P. (Coordinators), 2000 : Historical Tsunami Database for the US Pacific Coast (HUDBIUS) CDROM. Jointly produced by Intergovernmental Oceanographic Commission, US National Weather Service Pacific Region and Institute of Computational Mathematics and Mathematical Geophysics of the Siberian Division Russian Academy of Science, November 2000.

Hall, R., 1966 : Reconstructing Cenozoic SE Asia. In R. Hall and D. Blundell (Editors) "Tectonic Evolution of Southeast Asia". Geological Society Special Publication No. 106.

Hamilton, W., 1979 : Tectonics of the Indonesian Region. US Geological Survey Professional Paper 1078,345pp.

Hamzah, L. Puspita, N.T. and Imamura, F., 2000 : Tsunami Catalogue and Zones in Indonesia. Journal of Natural Disaster Service, 22, 1, 25-43.

Heck, N.H., 1947 : List of Seismic Sea Waves. Bulletin of the Seismological Society of America, 37, 4, 269-286.

Hedervari, P., 1984 : Catalogue of Submarine Volcanoes and Hydrological Phenomena Associated with Volcanic Events 15OOBC to December 21. 1899. US Department of Commerce, NOAA, National Geophysical Data Center, Boulder, USA, World Data Center A for Solid Earth Geophysics, Report SE 36,62pp.

Hedervari, P.. 1986 : Catalogue of Submarine Volcanoes and Hydrological Phenomena Associated with Volcanic Events January 1, 1900 to December 31, 1959. US Department of Commerce, NOAA, National Geophysical Data Center, Boulder, USA, World Data Center A for Solid Earth Geophysics Report SE-42, 35pp.

lida, K., Cox, D.C. and Pararas-Carayannis, G., 1967 : Preliminary Catalogue of Tsunamis Occurring in the Pacific Ocean. Hawaii Institute of Geophysics.

Lander, J.F. and Lockridge, P.A., 1989 : United States Tsunamis (including United States Possessions). US Department of Commerce, NOAA, National Geophysical Data Center Boulder, USA, World Data Center A for Solid Earth Geophysics Publication 4% 2, 265~~.

Lander, J.F.. Lockridge, P.A. and Kozuch, M.J., 1993 : Tsunamis Affecting the West Coast of the United States 1806-1992. US Department of Commerce, NOAA, National Geophysical Data Center, Boulder, USA, NGDC Key to Geophysical Records Documentation KGRD-29. December 1993,242~~.

Latter, J.H., 1981 : Tsunamis of Volcanic Origin - Summary of Causes with Particular Reference to Krakatoa, 1983. Bulletin Volcanologique, 44, 3, 467-490.

Lockridge, P.A. and Smith, R.H., 1984 : Map of Tsunamis in the Pacific Basin, 1900-1983. Scale 1:17,000,000. US NOAA National Geophysical Data Center World Data Centre A For Solid Earth Geophysics and Circum-Pacific Council for Energy and Minteralo Resources Map Project.

Otto, P.W. and Murty, T.S., 1996 : Predicted Tsunami Travel Time Charts for the Indian Ocean. National Tidal Facility, The Flinders University of South Australia, Adelaide, Australia, Publication, July 1996.

Pararas-Carayannis, G.. 1969 : Catalogue of Tsunamis in the Hawaiian Islands. US Department of Commerce, NOAA National Geophysical Center, Boulder, USA, World Data Center A for Solid Earth Geophysics Publication, 94pp.

Prasad, G., Rynn. J. and Kaloumaria, A., 2000 : Tsunami Mitigation for The City of Suva, Fiji. Science of Tsunami Hazards. 18, 1, 35-54.

Rynn. J. and Davidson, J.. 1999 : Contemporary Assessment of Tsunami Risk and Implications for Early Warning for Australia and Its Island Territories. Science of Tsunami Hazards, 17. 2, 107-125.

Simkin, T. and Seibert, L, 1994 : "Volcanoes of the World". 2"d edition, Smithsonian Institution Global Volcanism Program. Geoscience Press, Tucson, Arizona, USA, 394pp.

Solem, J.C.. 1999 : Comet and Asteroid Hazards Threat and Mitigation. Science of Tsunami Hazards. 17. 3, 141-153.

Soloviev, S.L. and Go, C.N., 1984 : Catalogue of Tsunamis on the Western Shore of the Pacific Ocean. Nanka Publishing House, Moscow, 1974. Canadian Translation of Fisheries and Aquatic Sciences No. 5077, 439pp.

Soloviev, S.L., Go, C.N. and Kim, K.S., 1992 : Catalogue of Tsunamis in the Pacific 1969 1982. Academy of Sciences of the USSR, Soviet Geophysical Committee, Moscow. Translated by Amerind Publishing Co. Pty Ltd, New Delhi, 208~~.

Tappin. D.R., Matsumoto, T., Watts, P.. Sataka. K., McMurty, G.M., Matsuyama, M., Lafoy, Y., Tsuji, Y.. Kanamatsu. T., Lus, W., Iwabuchi. Y.. Yeh, H., Matsumoto, Y., Nakamura, M., Mahoi. M,. Hill, P., Crook, K., Anton, L., and Walsh, J.P., 1999 : Sediment Slump Likely Caused 1998 Papua New Guinea Tsunami. Eos, Transactions, American Geophysical Union, 80, 30, 329-340.

REMOTE OPERATION OF THE WEST COAST AND ALASKA TSUNAMI WARNING CENTER

Alec H. Medbery, West Coast/Alaska Tsunami Warning Ctr./NWS/NOAA, Palmer, AK, USA

Guy W. Urban, West Coast/Alaska Tsunami Warning Ctr./NWS/NOAA, Palmer, AK, USA

Paul M. Whitmore, West Coast/Alaska Tsunami Warning Ctr./NWS/NOAA, Palmer, AK, USA

Thomas J. Sokolowski, West Coast/Alaska Tsunami Warning Ctr./NWS/NOAA, Palmer, AK, USA

ABSTRACT

The remote control of real time derivation of earthquake location and magnitude and the issuance of tsunami and earthquake bulletins was done using off-the-shelf remote control software and hardware. Such remote operation of the West Coast/Alaska Tsunami Warning Center can decrease the time needed to respond to an earthquake by eliminating travel from the duty standers' home to the tsunami warning center.

Science of Tsunami Hazards, Volume 20, Number 4, page 216 (2002)

Introduction

Presently, the West Coast and Alaska Tsunami Warning Center (WCATWC) in Palmer, Alaska operates with two staff members on standby duty within five minutes recall of the warning center during non-duty hours. The average time to respond to an earthquake, including travel, is about eight minutes. It is becoming necessary to decrease that response time in order to satisfy the needs of some users. To make this decrease more difficult to achieve, the ability of the duty personnel to respond within five minutes is hampered by the growth of traffic and traffic lights in Palmer, as well as winter driving conditions. The fact that there is not enough staff to man the center 365/24/7 is also a factor making a faster response time harder to meet. As in most organizations that use standby personnel on off-office hours, there is the period of travel to the office that must be included in the total response time. A possible solution to this dilemma is the use of remote control. This would eliminate the travel time in the total response time. Thus, possibly, allowing for a decrease in the response time needed to issue a tsunami bulletin.

Development

We started to investigate whether the initial warning messages could be issued from alternate locations, mainly home. With the explosion of high speed Internet, DSL, cable and wireless options we set down a few criteria:

1. The remote system must be able to completely solve the earthquake parameters.
2. It must be able to issue messages using the existing procedures.
3. It must do the above in real time.

The Internet was eliminated immediately as it is a public entity with no guarantee of reliability and raises many security concerns. The other options were a matter of speed and data handling capacity. Cable is available in Palmer but requires use of the telephone company server, which is a major reliance and security concern. This left us with DSL and wireless, which complement each other as backups to one another.

We started with the DSL, as it was the easiest to implement. Commercial DSL modems are readily available for a reasonable price. We settled on a SDSL two wire leased line network extender that is capable of 2.32Mb at a distance of 12,000 feet. Since all personnel live within five minutes already, telephone service to each house is within that distance and the local telephone utility will connect the shortest route possible on request. This is also a direct routing that may go through the telephone company central station, but not through their DSL server. Hence, it is essentially a direct connection from the WCATWC to each duty house.

For testing purposes we looped two pair of telephone lines through the Geophysicist-in-Charge's residence with a pair of extenders on each end. The output of the extender has a RJ45 LAN connector which we plugged into our operational LAN hub. The output of the other extender was connected to a laptop with a 10BASE-T Ethernet card. After setup, the laptop became an extension of our operational LAN with equal access to all

operational systems. Although we were able to access files, printers, communications ports, etc. there was no way we could run the operational software.

We then had the option of remotely running the operational software ON the laptop or running the operational software FROM the laptop. For the former, at the WCATWC, there are three Earlybird systems (Whitmore and Sokolowski, 2002) that can independently solve the earthquakes parameters and issue warnings. The outputs of these systems are "coupled" to the message dissemination systems, i.e. NWWS (NOAA Weather Wire), Nadin II (FAA), line 106 (backup NWWS), etc. so any Earlybird system can send to any or all message systems. For the remote to be fundamentally an Earlybird4, would require extra lines from the remote location to the message systems if the operational software were ON the laptop computer. Therefore, the latter option was selected, as additional communications links to the dissemination systems could be eliminated. Simply, we would control one or all of the existing Earlybirds remotely from the laptop. This had the added advantage of control or monitoring of all operational LAN computers via the remote laptop, including the EarthVu and Tide systems.

There are several remote control software packages available including freeware, shareware and commercial. Each has its own advantages, disadvantages, perks and quirks. After testing several of these, we found they all did a credible job, but only one had reliable documentation and a long history of use and progression; pcAnywhere from Symantec. Although there is a slight delay from keystroke to action, the software worked as desired allowing full control of any operational PC selected. Since we use NETBEUI protocol on the operational LAN, an added benefit was it worked noticeably quicker than when using TCP/IP.

It should be noted here that the computers Earlybird 1 and 2 have 6 monitors each and the computers EarthVu 1 and 2 have 4 monitors each. The computer, EarlyBird3, has just one monitor with all six windows on that single screen, see Figures A and B. The remote laptop computer has only one monitor, so control of the system is somewhat slower due to switching different screens in and out of view, similar to Earlybird3. Although six monitors could be installed at each remote location, cost would be a major factor. Also, the point of this project is to be able to initiate a warning from a remote location quickly; not totally control a warning from start to finish. Watch standers would still respond to the office after initial warning messages are disseminated.

Next we decided to try voice and video so watch standers could communicate, coordinate and confer during an event. Although there are commercial software vendors that offer these services, they are usually bundled with higher end programs for corporate Internet e-mail, point of sale, or database searches. Also, the high overhead slows down the operational software. WIN2K has a program called NetMeeting incorporated into the operating system that provided all the functionality we required. Unfortunately, it requires TCP/IP addressing to work, which forced us to change the pcAnywhere to TCP/IP, which, as mentioned above, slowed the response of the remote control software. Everything worked correctly, but keystroke to action time increased by a factor of at least two and we considered this too much lag time. At least until technology improves and/or becomes more cost effective, we believe that video, although nice, is not a necessity as is voice, and that voice should probably be handled separately through a radio link with the office. This would also provide us a two-way communications link for the stand-by

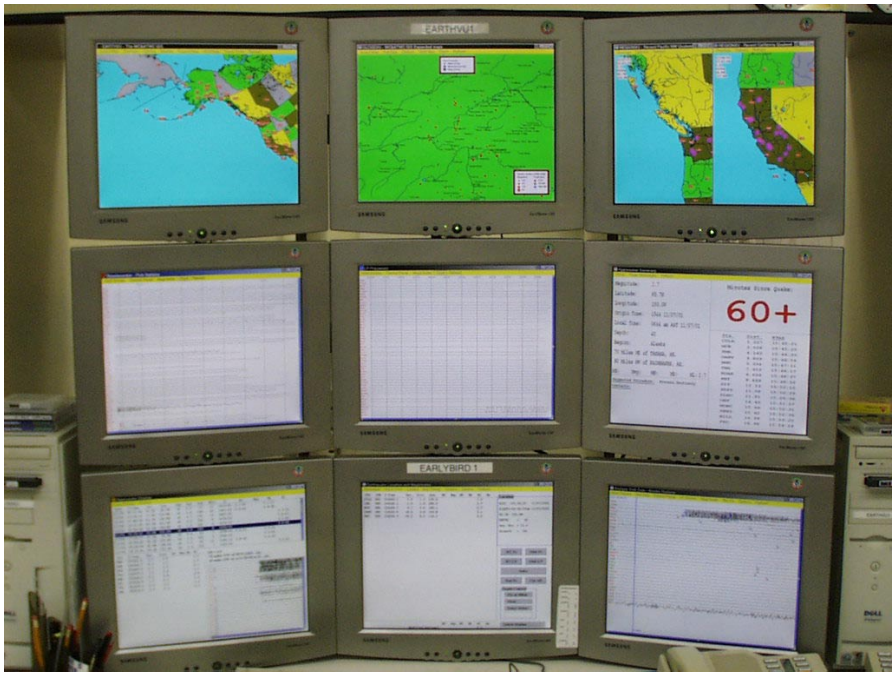

Figure A: EarlyBird1 consists of the bottom six monitors. The top three monitors are part of EarthVu1.

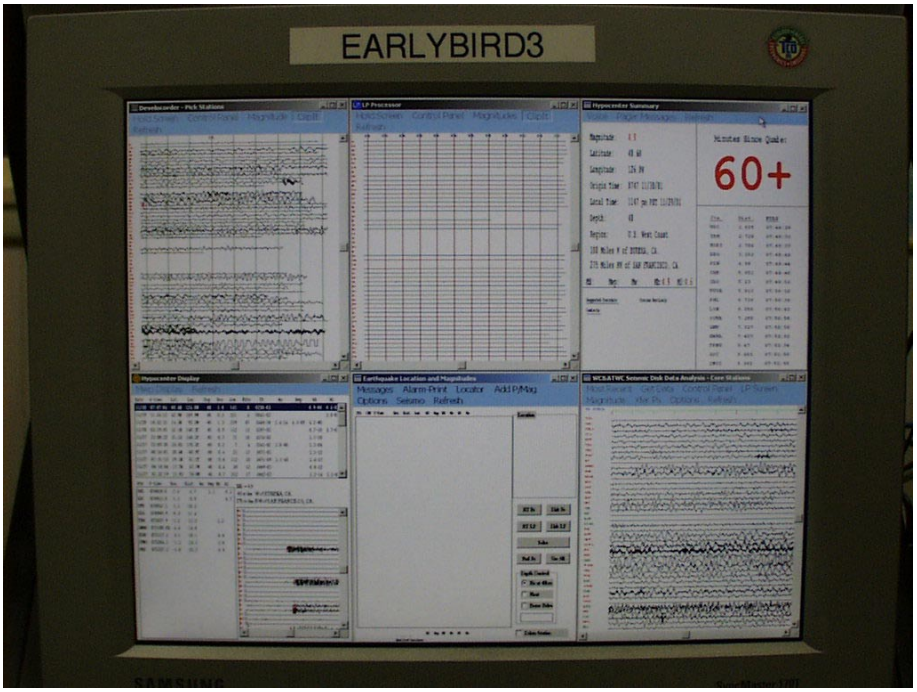

Figure B: EarlyBird3 consists of one monitor with all six programs on the same monitor.

personnel. It should be noted that alternatives for both voice and data are radio, cell phone, and satellite phone.

After successfully proving that running the seismic software remotely in real time by means of DSL is feasible, the next test was trying wireless as a backup to the remote DSL system. A Speedlan 4100 wireless system was tested. This system consisted of an Ethernet brouter and a unique pole-mount that allowed up to 300 feet of single Teflon jacketed cable to be run from the connection point of the network up to the RF device, without introducing loss of any radio signal. This RF device operates in the 2400 MHz to 2483.5 MHz ISM band and contains 11 user selectable RF channels. By placing one brouter at each of six WCATWC personnel's homes, a wireless network can be achieved. A line of site transmission is needed for the wireless LAN to function, since trees and building degrade or stop the RF signal. The maximum speed of transmission is 11 Mb with a maximum distance of 25 miles. No license is needed to run the wireless system and it has low power requirements. Again, we set up a test on the computer and were able to connect the remote PC to the operational LAN using the wireless interface. This was an ideal wireless link, i.e., no obstacles such as trees or buildings. It should be noted that it was beyond the scope of this test, to make wireless connections to the duty standers' homes, other than to the on site home of the GIC. Upon consulting with wireless engineers, they felt that to have success connecting the watch standers' homes could be limited due to terrain and obstacles in Palmer.

Discussion

We found that we were able to use a remote system via the operational LAN to completely solve for earthquake parameters such as location and magnitude. We also proved that we were able to issue messages from the remote PC in real time. Noticeable disadvantages for remote operation of the warning center are the inability to access the external National Warning System circuits and answering of phone calls. These problems can be overcome with the use of satellite, cell phones and radio. Even the use of video conference technology could arrest some of these disadvantages. All of the above would depend on security and reliability issues. If standards for these are relaxed to allow commercial carriers, then options in all areas dramatically increase. If the standards are not relaxed to allow commercial carriers, multiple (DSL, wireless, radio, and etc.) or "high end" systems would suffice. However, as stated earlier, the purpose of the remote system is speed up the issuance of the tsunami initial message products, not replace the entire message process. Other disadvantages are transmission path obstructions (trees, buildings and weather), security, external equipment on private homes (building code and covenant violations) and operations and maintenance of new systems in each person's home.

Using remote control could expedite the issuance of critical tsunami and earthquake messages. Delays in response time could be reduced with remote operation of the WCATWC. Eliminating the current travel time delays would be beneficial to the TWS geophysicist who must issue and conclude warnings and watches; and, for emergency officials who have the task of evacuating people or avoiding unnecessary evacuations. While all operational details of the conversion to remote operation of the WCATWC

have not been solved, remote control is shown to have the potential of reducing the issuance time of the initial tsunami warning bulletin.

Disclaimer

The conclusions and views expressed in this paper are solely those of the authors and not of the National Weather Service.

References

Whitmore, P.M. and Sokolowski, T.J.; Automatic Earthquake Processing Developments at the United States West Coast and Alaska Tsunami Warning Center, in Recent Research Developments in Seismology, in press, Transworld Research Network, Kerala, India, 2002.

PREDICTION OF SLUMP GENERATED TSUNAMIS: THE JULY 17TH 1998 PAPUA NEW GUINEA EVENT

David R. Tappin
British Geological Survey, Nottingham, UK
Philip Watts
Applied Fluids Engineering, Inc., Long Beach, Calif., USA
Gary M. McMurtry
School of Ocean and Earth Science and Technology, University of Hawaii, Hawaii, USA
Yves Lafoy
Services des Mines et de l'Energie, Noumea, New Caledonia
Takeshi Matsumoto
Japan Marine Science and Technology Center, Yokosuka, Japan

ABSTRACT

The local tsunami of July 17th 1998 that struck Papua New Guinea is most probably the result of an offshore sediment slump. This conclusion is based on multibeam bathymetric data, visual observation of the seabed, and sediment piston cores. Offshore data has been utilised to interpret the tectonic framework of the area off northern PNG, the local sedimentary regime and, from this and onshore evidence of sediment dispersal a model of sediment failure has been constructed. Utilising the seabed observations, the distribution of seabed failure has been mapped and the tsunami source location accurately identified. Fluid expulsion from the sediment has been assessed from the presence of authigenic carbonates and chemosynthetic communities. It is proposed that multibeam bathymetry, sediment sampling, and visual seabed observation are critical in the identification of coastlines vulnerable to tsunami attack and, in combination with onshore studies and numerical simulations, tsunami prone areas may be identified. Ultimately, as more case studies are undertaken, underwater landslide prediction may at last become possible.

INTRODUCTION

With the increasing availability of high-resolution multibeam-mapping systems, there is an expanding knowledge of detailed seabed morphology and the processes through which this morphology has formed. One aspect of this increased database is the recognition of submarine slump-created seabed features and their tsunamigenic potential. Seabed slump scars are now identified off of many coasts. Examples include: Alaska (von Heune et al., 1999), Chile (von Huene et al., 1997), the east coast of the United States of America (Driscoll et al., 2000), California (Orange et al., 1999) and the Ryukyu Islands (Matsumoto et al., 1997). Some of these slumps are located far from shore or in deep water and thus their tsunamigenic potential is limited. Others, however, are near to shore and their formation may well have generated a local tsunami that struck the neighboring coast. The most recent event is the Papua New Guinea tsunami of July 17, 1998 (Kawata et al., 1999; Tappin et al., 1999; Tappin et al., 2001).

The Papua New Guinea (PNG) tsunami brought the threat of locally generated tsunamis sharply into perspective when it was realised that the most likely cause was a sediment slump just offshore (Kawata et al., 1999; Tappin et al., 1999). Over 2,000 people died when the 10 m plus waves focused onto a short stretch of shoreline (Kawata et. al., 1999). Earthquakes are common along the north coast of PNG, but the tsunami was entirely unexpected given the main shock had a magnitude of 7.1. The impact on PNG was obviously considerable, but for many coastal communities worldwide it was a 'wake-up' call to the catastrophic threat of locally generated tsunamis.

The objective of this paper is to present a synthesis of the offshore data acquired after the 1998 PNG event and to consider how data of this type may contribute to the prediction of slump generated tsunamis. One of the challenges of tsunami science is to further understand the mechanisms of offshore sediment failure that may be tsunamigenic. Understanding how and why slumps occur will enable us to predict their occurrence, or at least to identify areas facing the greatest hazards. In the instance of PNG, there has been considerable debate over the source of the tsunami, although in the authors' view the offshore evidence confirms a slump source. Offshore data has proved invaluable in discriminating between alternative tsunami source mechanisms.

THE PAPUA NEW GUINEA TSUNAMI

The PNG tsunami attained a maximum height of 15 m with extreme focusing along the low-lying sand spit fronting Sissano Lagoon. The waves resulted in the loss of over 2,000 lives and the complete destruction of three villages with four more badly damaged.

A number of lines of evidence suggested that the tsunami was not the direct result of coseismic displacement but rather of a sediment slump. Survivors' accounts indicated that the wave arrived at the sand spit at or about the same time as the first strong aftershock or second earthquake (Davies, 1998). A tsunami wave originating from the main shock would have arrived (from an earthquake located ~20 km offshore) within ten minutes. The tsunami actually arrived twenty minutes after the main shock. Analysis of the earthquake frequency content showed the main shock not to be unusually tsunamigenic (Newman and Okal, 1998b). Mathematical simulation based on a dislocative source (Titov and Gonzalez, 1998; Newman and Okal, 1998b, Kawata et. al., 1999) recreated neither the maximum wave height nor the longshore wave height distribution.

An offshore survey was required to identify the tsunamigenic potential of the area offshore northern PNG and to discriminate between alternative tsunami source mechanisms. Bathymetric data would also be used to identify features that would focus waves onto the coast. The most likely alternative to a sediment slump was a steeply dipping reverse fault upthrust to the south

(Titov and Gonzalez, 1998; Newman and Okal, 1998b, Kawata et. al., 1999). An appeal by Alf Simpson, the Director of the South Pacific Applied Geoscience Commission (SOPAC), led to a response by the Japan Marine Science and Technology Center (JAMSTEC) that offered at least two offshore surveys. Based on the success of the first two surveys, a third survey followed.

Prior to these surveys, the area offshore of northern PNG was unknown in detail. Interpretation of regional gravity and bathymetric data showed a complex of microplates bounded by shallow trenches (Figure 1). The geological evolution of the area is interpreted as a series of collisions along the northern margin of the Australian plate that has resulted in suturing of island arc and oceanic terranes along the northern part of PNG (Cooper and Taylor, 1987; DeMets et al., 1994; Crowhurst et al., 1996; Stevens et al., 1998; Tregoning et al., 1998).

THE OFFSHORE SURVEYS

Two surveys were initially planned by JAMSTEC and SOPAC, and took place between January and March, 1999. A third JAMSTEC/SOPAC survey took place in September 1999. The survey objectives were to provide a regional geological context to the tsunami source mechanism, to identify possible tsunami sources, and to acquire detailed bathymetry for numerical simulations. Participating scientists formed a multidisciplinary and multinational group.

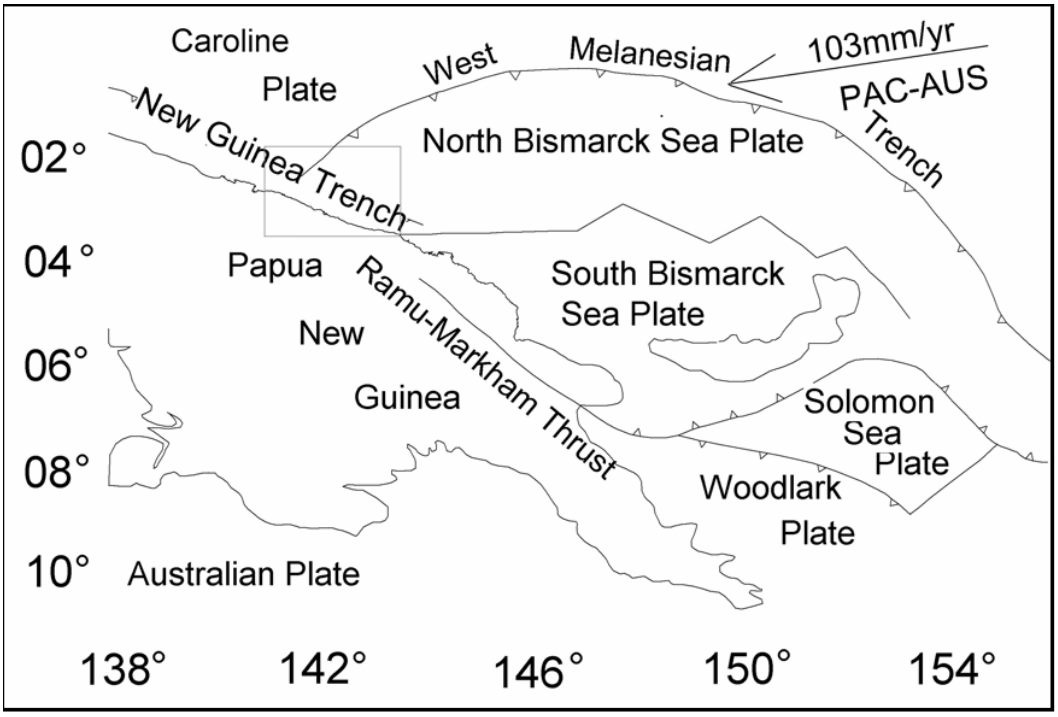

Figure 1: Plate tectonic setting of Papua New Guinea, with main microplates named. Arrow shows convergence azimuth of the Pacific (comprising the Caroline and North Bismarck Sea plates) and Australian plates. Box indicates the area of the bathymetric map shown in Figure 2.

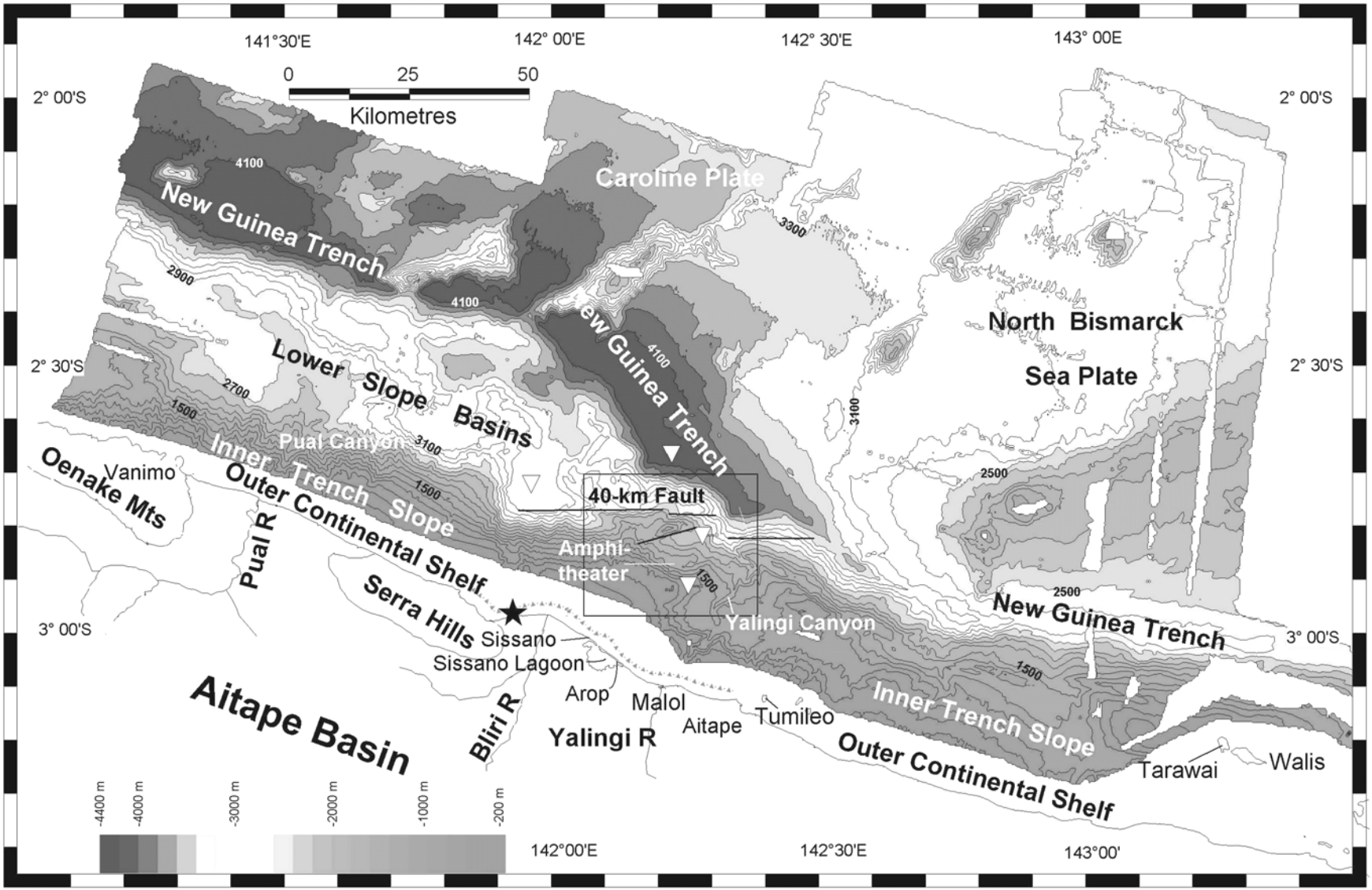
141°30'E
142° 00'E
142° 30'E
143° 00E
0
25
50
Kilometres
2° 00'S
2° 30'S
3° 00'S
Caroline Plate
New Guinea Trench
North Bismarck
Sea Plate
Lower Slope Basins
Pual Canyon
Inner Trench Slope
Outer Continental Shelf
Oenake Mts
Vanimo
Pual R
40-km Fault
Amphi-
theater
Yalingi Canyon
New Guinea Trench
Serra Hills
Sissano
Sissano Lagoon
Aitape Basin
Bliri R
Arop
Malol
Aitape
Tumileo
Yalingi R
Inner Trench Slope
Outer Continental Shelf
Tarawai
Walis
4100
3300
2900
2700
3100
2500
1500
-4400 m
-4000 m
-3000 m
-2000 m
-1000 m
-200 m
142°00'E
142°30'E
143°00'

Facing page. Figure 2. Bathymetry and main morphologic elements offshore of northern Papua New Guinea together with the main coastal locations and features. Filled triangles identify the area devastated by the 17th July 1998 tsunami. Black star is the most likely epicentral location of the 17th July 1998 earthquake. Open triangles are Sediment Core locations. Box is the area of Figure 3. Contour interval of 200 meters.

The first survey acquired 19,000 km2 of multibeam bathymetry, 4.2 khz high-resolution subbottom seismic lines, and four 8 m long sediment piston cores. Gravity and magnetic data were also acquired. The second survey utilized the tethered Remotely Operated Vehicle (ROV), the Dolphin 3-K, to acquire seafloor images using VCR and still photos together with rock samples and short (30 cm) push cores. The third survey utilized the manned submersible (MS), Shinkai 2000 and acquired further VCR images, still photos and rock and sediment samples.

SURVEY RESULTS

Bathymetry

The multibeam bathymetry reveals a complex morphology offshore northern Papua New Guinea (Figure 2). There is the New Guinea Trench, along which the Pacific Plate is being subducted southward beneath PNG. Along strike (east to west) there are morphological changes of the New Guinea Trench that may be traced from the inner trench wall to the Pacific Plate.

To the east of Sissano Lagoon, the inner trench slope is narrow at 15 km with steep gradients. The lower part of the slope is deformed mainly by strike faults. To the west, the inner trench slope increases in width to 25 km, and at the foot of the slope lie a series of lower slope basins with steep upper scarps and backtilted basin floors. The inner slope is dissected by two deeply incised submarine canyons together with numerous smaller canyons that are especially concentrated along the subsided delta front off Sissano (see below). The two larger canyons are offshore continuations of the Pual River in the west and the Yalingi River in the center.

Offshore of Sissano Lagoon, there is an area that is transitional in morphology between the areas to the east and to the west (Figure 3). Here, there is a subsided delta, on the northeast margin of which is located a reef at 500 m water depth. Below the reef lies an arcuate depression, termed the amphitheater. The amphitheater is bounded to the north by an upraised block. The Upraised Block is bounded to the south by an ESE-WSW trending fault (termed here the 14-Kilometer Fault) and the northern margin by an east-west trending normal fault (termed herethe 40-Kilometer Fault). The 40-Kilometer Fault extends westward from the New Guinea Trench to the most easterly of the lower slope basins. It downthrows to the north. In a westerly direction, it is progressively offset northward by a series of north to south trending minor faults. More arcuate structures are present at greater water depths towards the New Guinea Trench.

The east-west variations observed along the inner slope of the New Guinea Trench are reflected in the structure of the Trench and the Pacific Plate to the north. In the east, the Trench trends East to West, is shallow at 3,000 m and V-shaped. Below Sissano, to the west, there is an offset to the north, the trend changes direction to NW-SE, and the Trench becomes planar floored. The depth increases to 4,000 m. Further west, the trench trend becomes ESE-WNW although the trench floor morphology remains planar and at a depth of 4,000 m.

The Pacific Plate comprises two distinct plates along this margin: in the east, the North Bismarck Sea Plate, and in the west, the Caroline Plate. The former is at a shallower depth than the latter, cresting at 1,400 m and appearing to ‘carve’ into the eastern part of the inner trench wall. There is an arcuate boundary with the Caroline Plate segment along which water depths increase. On the Caroline Plate there are NE-SW trending arcuate chains of seamounts.

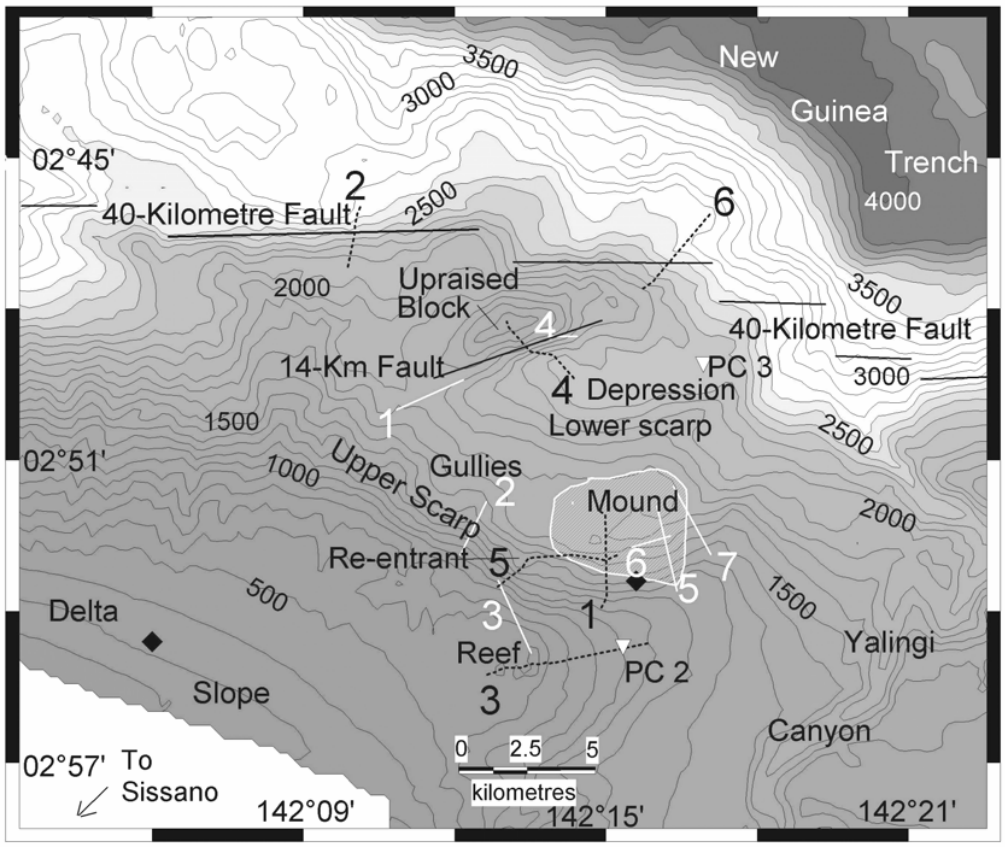

Figure 3. Amphitheater area off of Sissano Lagoon (located in Figure 2) with main morphologic features. Solid black lines are faults; hachured area defines the slump area of July 1998; dashed white lines are ROV traverses; solid white lines are Manned Submersible traverses; white filled triangles are sediment core locations; black diamonds are the two main aftershock locations. Contours at 100 meters.

Sediment Piston Cores

Four piston cores, each approximately 8 m long, were acquired. Three (PC-1, 3 and 4) are located in bathymetric lows and one (PC-2) below the subsided reef. Of the former three, one core was located in the New Guinea Trench to the north of Sissano, one in the depression at the foot of the amphitheater, and one in the easternmost lower slope basin. All cores in the depressions sampled olive-green, soft hemipelagic clays with interbedded silt-grade turbidites. The core at the foot of the subsided reef sampled 8 m of olive green, stiff, cohesive clay.

INTERPRETATION OF THE DATA FROM THE FIRST SURVEY

A number of significant results from the first survey informed us of both the overall structural framework as well as the sedimentary regime in the area. Interpretation of the bathymetry and core data disproved many of our previously held ideas. Undoubtedly, the area is an active convergent margin system, but contrary to our original ideas it is relatively sediment starved compared to nearby margins (e.g., the Sepik River delta). Both these conclusions are of importance in the assessment of tsunami hazards.

The varied morphology of the area is attributed to the subduction of the two (different) segments of the Pacific Plate. The Pacific Plate is moving west and the Australian/PNG Plate is moving north, resulting in a reported azimuth of convergence of ~070° (DeMets et al., 1994; Stevens et al., 1998; Tregoning et al., 1998). The convergence results in transpression along the margin with the westward moving and shallower North Bismarck Sea Plate acting as a 'snow-plough' that is tearing out the base of the inner trench wall through a process termed 'subduction erosion' (von Huene and Scholl, 1991). In the east, this results in subsidence of the inner trench wall along with the steep gradients and the dominant strike-slip faulting observed in this area. West of Sissano Lagoon, the subduction of the deeper Caroline Plate appears to result in a lesser amount of subduction erosion and a wider inner trench wall, although the gradients along the upper part of the inner trench wall are still steep. Faulting is dominantly normal, dip-slip, and results in the formation of the observed back-tilted lower slope basins. The difference in deformation between the east and west is attributed by Tappin et al. (2001) to the different crustal structure of the North Bismarck Sea and Caroline plates. The former is suggested to be less dense (and hence shallower than the latter) because of its formation by a combination of 'younger' backarc basin and island arc processes whereas the latter is older (~30-40 my), denser, and truly oceanic. The subduction of different crust with different densities results in the features observed.

The transitional area lies between Sissano Lagoon and the junction between the North Bismarck Sea Plate and the Caroline Plate (Figure 3). The result is a more complex morphology of normal faults and 'amphitheater' shaped depressions. The amphitheaters are considered to have formed by sediment slumping. Faults and arcuate amphitheater features appear to become older with depth. Convincing support for the interpretation of a subsiding inner trench wall, and proof that subsidence extends to shallow water depth, is provided by the subsided reef at 500 m (Figure 3). Samples obtained from the reef prove that it formed within the intertidal zone (Tappin et al., 2001). Onshore, the Sissano Lagoon formed by subsidence in 1907 (Neuhauss, 1911; Welsch, 1998), with subsidence continuing to the present day (Goldsmith et. al., 1999).

The amphitheater below the subsided reef is considered to be the most likely location for a recent sediment slump. A number of shallow gradient benches on the amphitheater evidence rotational faulting and the morphology suggests that the amphitheater may be the result of more than one slump event. A multichannel seismic line across the eastern part of the amphitheater provides evidence of a slump (Sweet and Silver, 2002). The 40-Kilometer Fault that marks the amphitheater's northern boundary displays normal (dip-slip) throw to the north.

The large, incised submarine canyons, together with the complex of small canyons on the submerged delta front off Sissano, suggest that there is little sediment being discharged into the amphitheater from land. Correlation with onshore drainage patterns show that the two major canyons are offshore extensions of two (Pual and Yalingi) of the three major rivers draining the adjacent land area. The third river, the Bliri, ends in the swamps and lowlands surrounding Sissano Lagoon and very little sediment or water is issuing seaward at the river mouth. The subsiding Sissano area is thus a sediment trap. The sediment deposited offshore is dependent upon the seabed gradient; thus, soft hemipelagic mud and turbidites accumulate in depressions whereas stiff cohesive sediments are exposed on the steep slopes. We await dating of the cores to estimate sedimentation rates in the area.

The main conclusion drawn from the multibeam and sampling survey is that the most likely source of the 1998 tsunami was in the vicinity of the amphitheater below the subsided reef. If the tsunami were due to a slump in this area, then the slumping mechanism would most likely be by rotational faulting in the stiff, cohesive clays similar to those sampled at the foot of the subsided reef. The fault on the northern margin of the amphitheater is considered an unlikely source of the tsunami because it is a normal fault with downthrow to the north. A reverse throw

(to the south) is required if the observations of a leading depression wave reaching the shore are correct (Kawata et al., 1999).

The results of the multibeam survey identified the 40-Kilometer Fault and the amphitheater as the prime targets for visual operations by the ROV and MS surveys to follow (Figure 3).

VISUAL OBSERVATIONS

The aim of the ROV and MS operations were to identify and observe seabed features that may indicate recent seabed movement resulting either from earthquake shaking (and associated faulting) or seabed sediment slumping. There were six dives using the Dolphin 3-K and seven using the Shinkai 2000.

Potential evidence of recent seabed movement includes fresh rockslides or talus slope deposits, sediment fissuring, fault scarps, and evidence of venting. Although there is no method by which these features, if present, can be dated, it was anticipated that temporal relativity could be gauged by their state of preservation.

The Amphitheater

Two ROV dives (1 and 5, Figure 3) located on the upper scarp face of the amphitheater identified extensive fissuring in the cohesive clays (Figure 4 a, b and c). Individual fissures are over 50 m long, two to three meters wide and similarly deep. The fissures largely follow the depth contours of the amphitheater. Soft sediment overlying the cohesive clays is centimeters deep, confirming the conclusions drawn from the multibeam survey about low sedimentation rates on the steep slopes. The fresh appearance of the fissures (sharp, vertical sides, minimal sediment infill, and no evidence of sidewall collapse) all suggest a recent origin. ROV dive 1 encountered a 10-15 m high vertical headwall that is interpreted as an upper detachment of a sediment slump (Figure 4 d and e). Vertical color variation in the soft sediment at the surface from yellow-brown to lime green at depth suggests that the exposure time at seabed had not been long (yellow-brown sediment has been oxidised). At the foot of the amphitheater, there are bacterial mats and tubeworms (Figure 4 f) the presence of which is indicative of fluid venting. At the western end of the amphitheater (observed on ROV dive 5) there is a 30-40 m cliff comprised of exposed limestone (Figure 4 g), at the foot of which is a thick talus slope deposit of angular limestone blocks (Figure 4 h).

MS Dive 2 (Figure 3) to the west of the limestone cliff also located fissures in the cohesive sediment (Figure 5 a and b) as well as slumped decimeter sized cohesive sediment blocks. The sediment surfaces are degraded however and the features considered not of recent formation. The surface of steeply dipping cohesive sediment observed in a gully is also degraded. Three MS Dives (5, 6 and 7, Figure 3) on the eastern side of the amphitheater located numerous fissures with sharp defined margins. The fissures are associated with slumped limestone blocks (Figure 5 c, d, e and f), sulfide rich sediment (Figure 5 g), common chemosynthetic fauna such as tubeworms, mussels (*bathyiomodiolus* sp?) and bacterial mats (Figure 5 g and h and Figure 6 a) as well as signs of active fluid expulsion (shimmering in the water column). Many of the mussels are displaced downslope and may lie either within or on the sediment

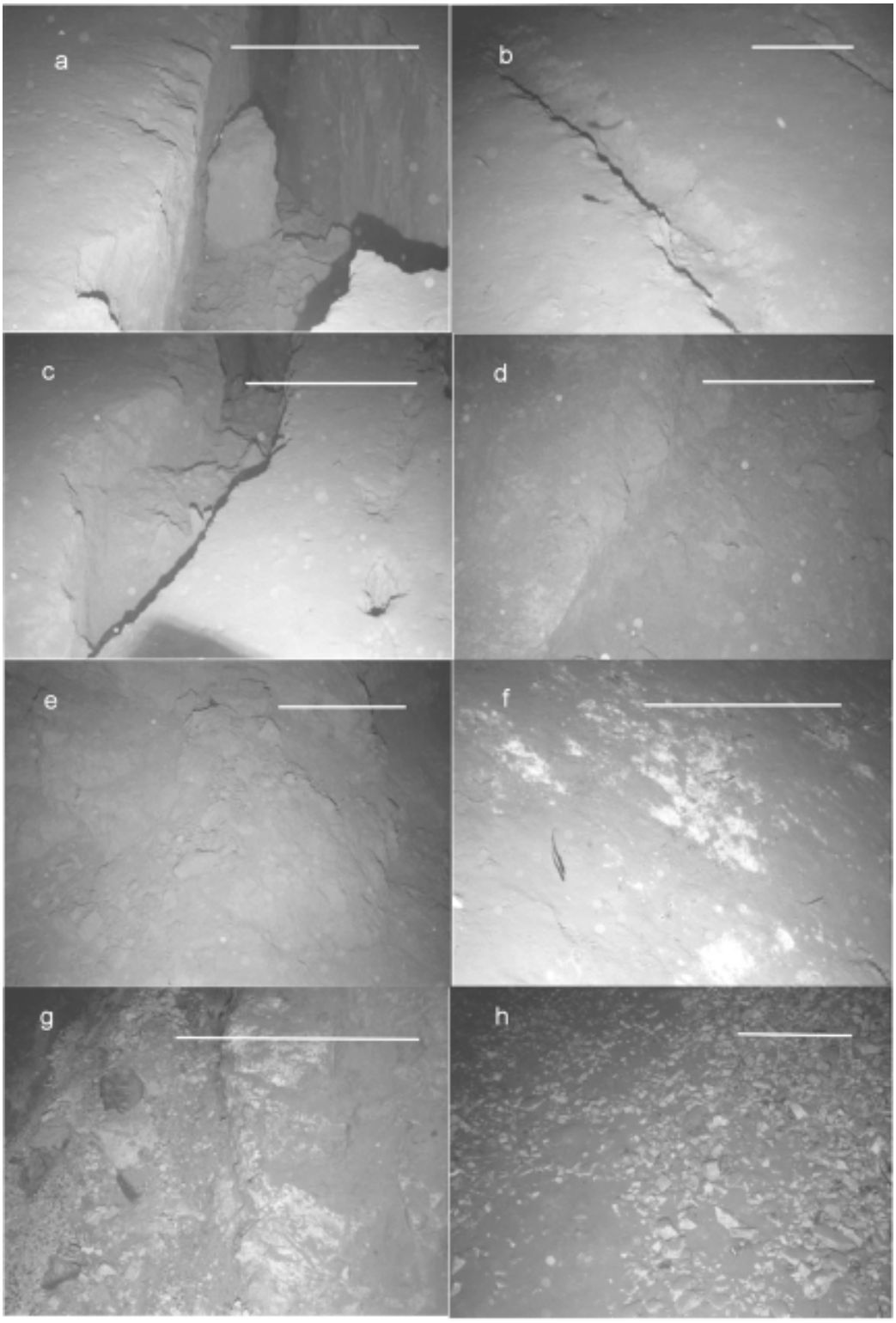

Figure 4. Photographs of upper scarp of amphitheater: a, b, and c; fissures in cohesive sediment: d and e; upper detachment on ROV 1 traverse: f; bacterial mats: g; limestone cliff on ROV 5 traverse: h; talus blocks below limestone cliff. Scale bar is one meter long.

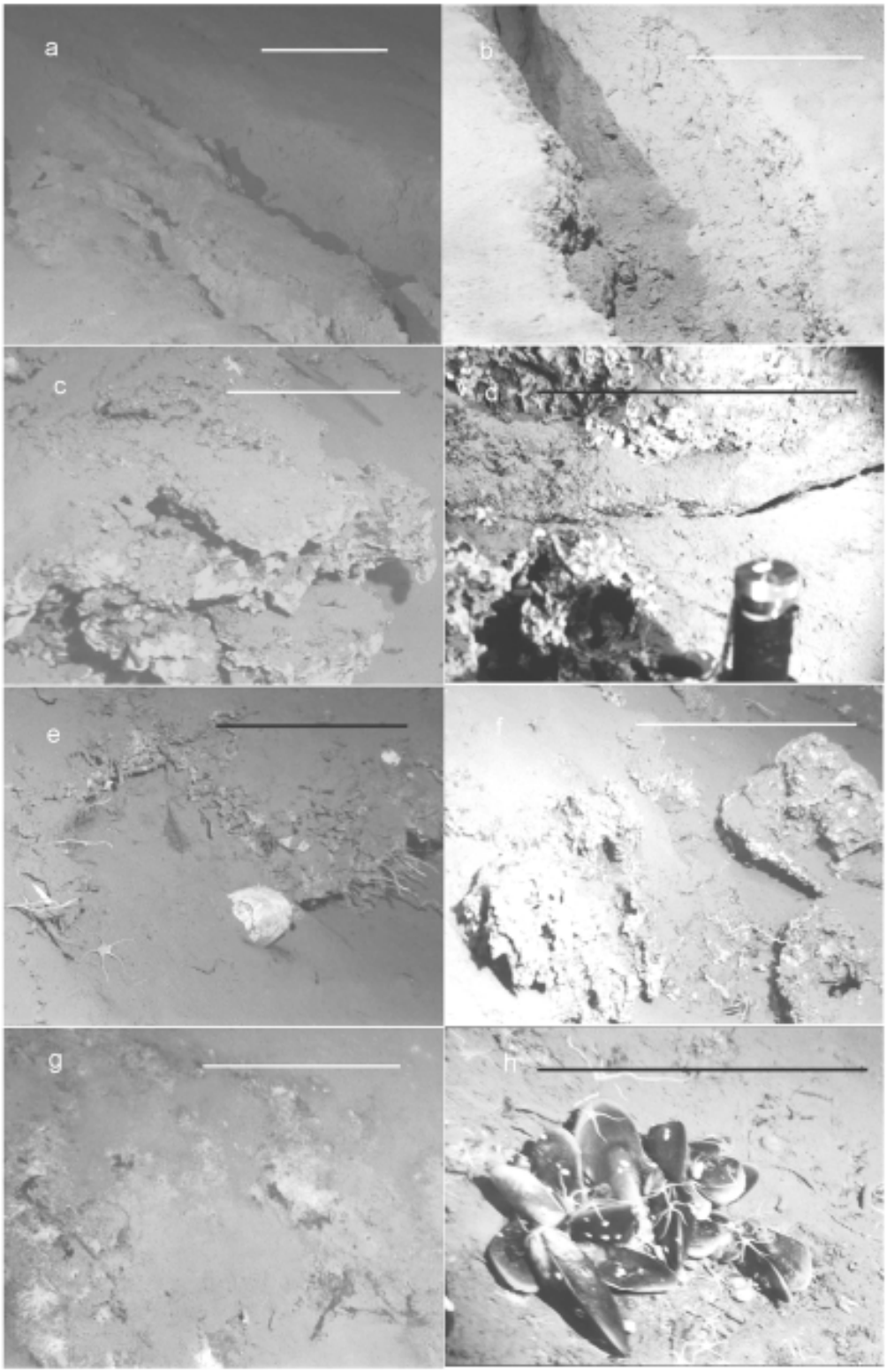

Figure 5. Photographs of upper scarp of amphitheater: a and b; fissures in the west: c, d, e and f; slumped vuggy limestone blocks with in 'e' slumped mussel shell and tube worms: g; sulfide rich sediment (black) and bacterial mats (white): h; mussels and starfish on sulfide rich sediment. White line is one meter. Black line is 0.5 meters.

(Figure 5 e, Figure 6 a). Along the upper margin of the amphitheater, a detachment surface or headwall provides evidence of the lateral extent of the slump (Figures 6 b and c). At the foot of the amphitheater, located on a ~4 km^2 mound (Figure 3) that appears to be the primary slump mass, there are numerous fissures (Figure 6 d). The disposition of these fissures suggests thrusting from the south (Tappin et al., 2001).

The subsided reef

ROV dive 3 on the subsided reef confirmed the origin of this structure. Samples proved the reef to be of intertidal origin (Figure 6 f); thus 500 m of subsidence had taken place since reef formation. A prolific chemosynthetic community of *bathymodiolus* sp? and tubeworms (Figure 6 e) confirmed that active fluid venting is taking place along the top of the continental slope.

The Upraised Block

Observation by both ROV (Dive 4) and MS (Dive 4) of the southern wall of the upraised block identified slump and fault scars (Figure 6 g) and loose blocks that formed talus slope deposits (Figure 6 h). The blocks are decimeter size with many are rounded although some are angular. There is not the overall appearance of freshness seen in the blocks at the foot of the limestone cliff at the amphitheater (compare Figures 4 h and 6 h). Seabed gradients are steep, in many places vertical to overhanging (Figure 7 a). An apparent fault (the 14-Kilometer Fault, Figure 3) running along the base of the upraised block showed evidence of recent vertical displacement of at most a decimeter.

The 40-Kilometer Fault

Two ROV dives on the fault to the north of the upraised block (Figure 3) illustrated significant variation along this feature. In the west (MS Dive 2), there is an exposed rock face (Figure 7 b) with talus slope deposits at its foot (Figure 7 c). Some rock debris was angular and therefore recently formed, but many rounded boulders (Figure 7 c) gave the appearance of age. There is no evidence of reverse fault movement; the movement is dip-slip or normal with downthrow to the north. MS Dive 6 located on the east of this feature discovered exposed rock only at shallow depth (Figure 7 d) and the seabed was found to be mainly sediment covered with little disturbance.

Overall, the amphitheater area showed the most evidence of seabed movement in both rock and cohesive sediment. The most common and active disturbance was located in the east. Fresh, sharp fissure boundaries, and angular slipped sediment and rock blocks suggest recent movement. Movement on the 40-Kilometer Fault and on the southern margin of the upraised block is minimal.

DISCUSSION OF THE OFFSHORE SURVEY RESULTS

Seabed investigation using multibeam bathymetry, sediment coring, and rock sampling together with visual observation using ROV and MS demonstrate that the most likely source of the July 17, 1998 PNG tsunami was a slump within the amphitheater sediments (Tappin et al., 2001). Slump width is widest at ~5 km and ~5 km long. Applying a typical 15% maximum thickness to length ratio, the 5 km length dimension indicates a slump thickness of ~750 m (Schwab et al., 1993; Turner and Schuster, 1996). This thickness is supported by the seismic data of Sweet and Silver (2002). The alternative fault source mechanism is not supported because the 40-Kilometer Fault is normal with downthrow to the north and is only active along its western segment. To be the tsunami source, the fault would have to be a reverse fault, with an overthrust

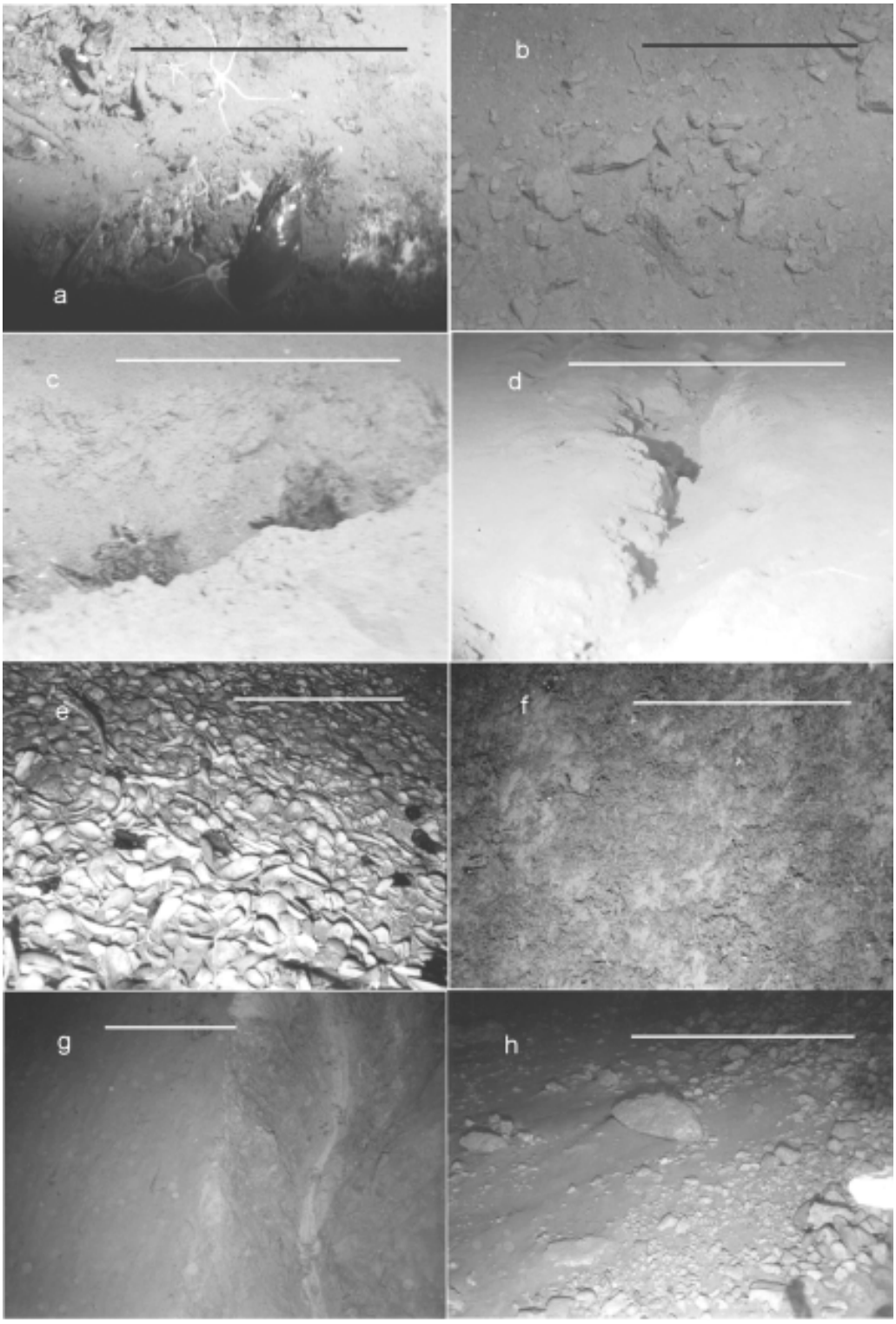

Figure 6. Photographs of -- Amphitheater eastern upper scarp: a; slumped mussel shells: b; loose sediment blocks on upper detachment: c; fissure at the top of upper detachment: d; fissure on mound at base of upper scarp – Subsided Reef: e; tube worm and mussel bed: f; acropora field – Upraised Block: g; fissure in sediment and rock: h; talus blocks. White line is one meter. Black line is 0.5 meters.

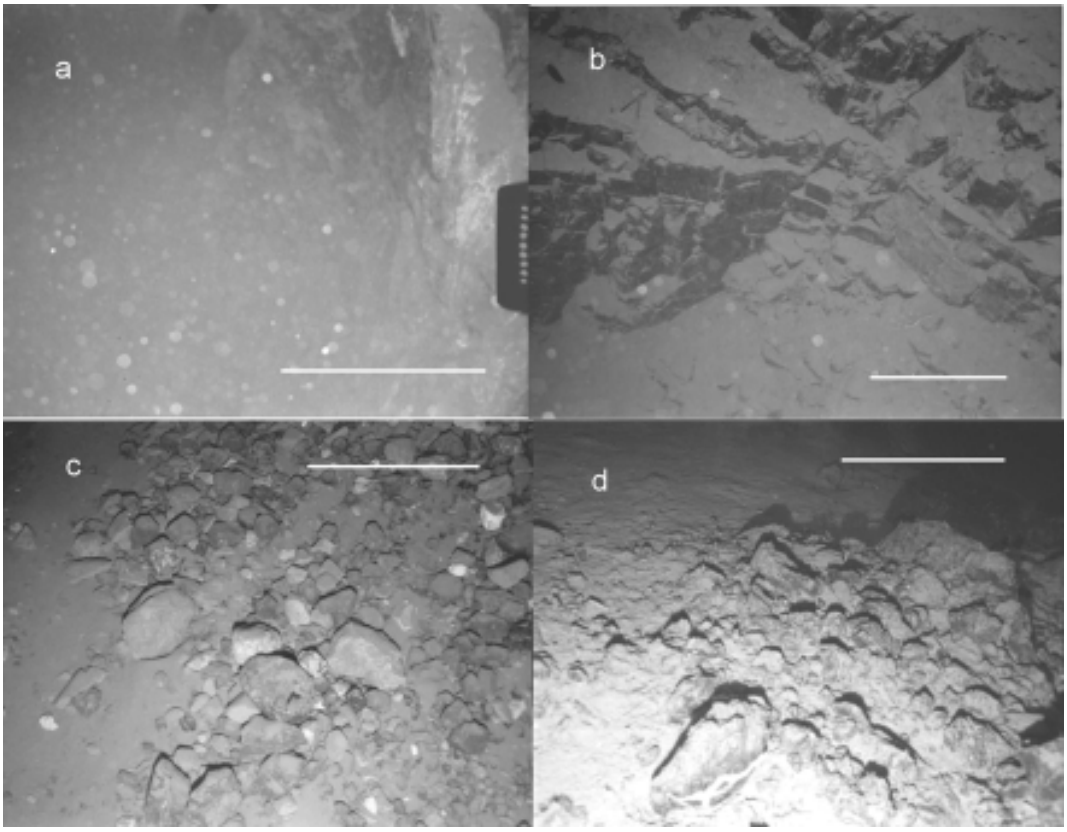

Figure 7. Photographs of -- Upraised Block: a; vertical ?fault face -- 40-Kilometer Fault on western segment: b; exposed fault face: c; rounded cobble boulders: d; weathered cobbles on the eastern fault segment. Scale bar is one meter long.

to the south, and be active along its entire length. A blind thrust (a thrust that does not cut the seabed) is also unlikely as there is no seabed manifestation of a thrust at depth.

Recent slumping within the amphitheater is strongly supported by the fissuring, the upper detachments or headwall, and the fluid venting. The upper detachment of a slump was observed on two dives. The slump is interpreted to lie in the east of the amphitheater in the area where the fissures are most numerous and where there is active fluid venting with associated chemosynthetic faunas. The slump was activated by rotational faulting (or crack propagation) in cohesive sediment rather than translational sliding in softer sediment. The fissures along the amphitheater are interpreted as formed by extension as the slump moved downslope. Fissures on the Mound proper are compressional features formed by upthrusting in the lower part of the slump. The multichannel seismic line acquired over the eastern part of the amphitheater supports this interpretation and suggests a slump volume of around ~6 km^3 (Sweet and Silver, 2002).

Dating of the sediment slump at present can only be attempted by comparing the morphologies of the observed features. The sharpest fissure edges are in the eastern half of the amphitheater. Those in the west are degraded and therefore considered ‘older’ by comparison. The increase in chemosynthetic faunas together with active venting towards the east also suggests this area to be presently (and most recently) active. To actually pinpoint the time of failure, we are now attempting to date the mussel shells sampled from the eastern part of the headwall. Tappin et al. (2001) suggest that the slumping led to increased fluid expulsion resulting in the post-slump population explosion in the biotas observed. The size of sampled mussel shells and published

growth rates support our conclusion that a slump mainly located in the eastern amphitheater was the source of the July 17th tsunami.

The presence of a slump in the eastern part of the amphitheater is also supported by the increase in sediment thickness in an eastward direction. Observations from the diving surveys suggest that sediment thickness is greater in the east because bedrock is exposed along the western part of the amphitheater but not in the east. The slump is located in an area of thick sediment accumulation (as also shown by the multichannel seismic lines acquired by Sweet and Silver, 2002).

The lithology (or strength and composition) of the sediment is important in tsunami generation because it controls the failure mechanism that in turn controls the magnitude of the tsunami wave generated. For example, failure of stiff clay is more likely to be tsunamigenic than failure in soft sediment (Turner and Schuster, 1996; Watts and Borrero, 2001). Thus, it is necessary to explain the sedimentary regime operating in an area and to describe the overall depositional environment from land to sea. In northern PNG, there are three main river systems that flow northward to the sea. Two, the Pual and Yalingi, flow directly into the incised submarine canyons observed on the inner trench slope. The third, the Bliri, terminates in a complex of swamps surrounding Sissano Lagoon. There is little egress to the sea. A range of mountains (the Toricelli-Bewani) that lie close to the coast limits the catchment area of the three named rivers. The main drainage of northern PNG is by the eastward flowing Sepik River that lies south of the Toricelli-Bewani Mountains. The Sepik discharges into the sea much farther east. The limited fluvial system around Sissano Lagoon explains the low sediment input offshore into the area of the survey. The fine clays, subsidiary silts, and sand turbidites sampled in the cores are the product of tropical weathering onshore.

Okal (1999) showed that the slump failed about 12 minutes after the main shock, ruling out ground acceleration as the cause of failure. Thus a mechanism is required to account for the delay in failure. The sediments we sampled were stiff and normally to slightly overconsolidated (Tappin et al., 2001). We therefore discounted a disentegrative (turbidity current) mechanism of tsunami generation. The retention of internal sediment structure (shown in the seismic profile of Sweet and Silver, 2002) also discounts this mechanism. Pore water migration in the impermeable, stiff clay would be slow and unlikely to induce failure after such a short period of time. Fluid pathways would be more likely to be within more porous/permeable layers (such as the vuggy limestones we sampled) in the slumped mass, along the basal sediment/bedrock interface (the zone of decollement identified on the seismic data), or along faults. The average shear strength estimated along the slump failure plane is an order of magnitude smaller than would be expected for stiff clay at the known failure depth (Watts and Grilli, 2002). Some other mechanism must account for the delay in failure.

Watts et al. (2002) calculate vertical coseismic displacement from the main shock using the shallow-dipping focal mechanism solution and an epicentre near the shoreline. They reproduce the subsidence of Sisanno Lagoon (as measured by McSaveny et al., 1999) and uplift of the Upraised Block. We suggest that the stress gradient within the overlying plate pumped water through the fault system from compressive towards extensional regions. The amphitheatre lies above the strongest stress gradients resulting from the earthquake main shock (and therefore the strongest water advection). We suggest that the stress difference following the main shock resulted in high-pressure water being pumped into and along the control fault (proposed by Tappin et al., 2001) that lies along the amphitheatre headwall. The water flow may have abutted against and then destabilised the sediment mass in the eastern part of the amphitheatre. High pressure water facilitates hydrofracture and crack propagation that may lead to mass failure, especially when initiated at depth beneath a sediment mass (Martel, pers. com.). The water located at depth also lubricates slump motion and may explain the low inferred shear strength of the stiff clay along the failure plane. Based on this failure scenario, the twelve minute delay between the main shock and sediment failure represents the advection time of the water from

depth to the slump failure plane. Slumping of the cohesive clays resulted in the internal faulting observed which facilitated fluid escape from both within and beneath the slump. The manifestation of the fluid escape is the chemosynthetic faunas and fluid expulsion features such as the shimmering in the water column. The venting is ongoing as pore water pressures around and within the mobilized sediment slowly return to equilibrium.

There is an interesting symmetry at play in the 12 minute delay between the main shock and the slump, versus the 8 minute delay between the slump and two strong aftershocks that occurred almost simultaneously 20 minutes after the main shock. One may readily calculate that slump displacement released as much potential energy as the main shock released in elastic energy. The slump lies directly above the epicenter of the eastern aftershock. We hypothesize that the slump triggered both aftershock events, a readjustment of elastic energy that is know to happen following rapid mass displacement. Roughly 1% of the slump potential energy change was released during the two strong aftershocks. We further speculate that the 8 minute delay may also be explained by the advection of water through fault systems leading down to the subduction zone. The aftershocks may have occurred along secondary thrust faults or at the subduction boundary.

CONCLUSIONS

With our experience of the PNG offshore surveys, we have no doubt of the importance of offshore data in the elucidation and validation of possible tsunami source mechanisms, whether these may be coseimic displacement or sediment slump. In the context of prediction, multibeam bathymetry provides data critical to the identification of offshore seabed features such as slumps and faults that in their formation may have been (and could potentially be) tsunamigenic. With the availability of high-resolution bathymetry, detailed knowledge of possible source locations improves the accuracy of numerical simulations. In the instance of PNG, an unusually large local tsunami has been demonstrated to be the probable result of sediment slumping together with bathymetric focussing. The location of the tsunami source determines both the magnitude and the focussing of the tsunami wave(s). A full fluid dynamic simulation of tsunami generation, knowledge of the exact location of the source, and detailed bathymetric data provide the most realistic numerical simulation of the event to date (Tappin et al., 2001).

In the wider context, consideration of both onshore and offshore morphology allows sedimentation patterns to be elucidated, enabling an evaluation of the tsunamigenic potential of extant sediments. Offshore Sissano Lagoon, moderate rates of sedimentation were interpreted from the multibeam data (further demonstrating the value of this data set). Piston coring proved the sediments on the steeper slopes to be stiff and cohesive. Sediment stiffness was a critical factor in the mode of failure (rotational slumping rather than translational sliding or turbidity flow in fluidized sediment) and therefore controlled the transfer of energy into the water column during tsunami generation. Mass movement center of mass motion has a significant effect on tsunami amplitude and wavelength (Watts and Grilli, 2002). Certain sediment characteristics, such as sediment cohesion, can be important predictors of mass failure and tsunami generation (Watts and Borrero, 2001).

Fluid content of the sediment also directly affects sediment stability. For example, off the East Coast of the USA, rapidly deposited and undercompacted sediments are considered likely to fail because of fluid overpressure (Dugan and Flemings, 2000). Large scale fissuring may provide visual evidence of pending slope instability (Driscoll et al., 2000). In contrast, mass failure in the instance of the PNG slump was entirely different, as the sediments are impermeable stiff clays, and failure is attributed to the injection of pressurized fluid. Offshore PNG, diffuse and low levels of fluid expulsion are evidenced by the presence of authigenic carbonate. Increasing levels of expulsion result in bacterial mats, clams and mussels and tubeworms, and ultimately the observed shimmering in the water column. The catalyst to failure may be stress variations as

opposed to earthquake ground shaking. In either case, chemosynthetic communities may be indicators of failure prone sediments (Tappin et al., 2001). Slumping may be caused by a transient water pulse and hydrofracture, whereas slumped sediment becomes a longer-term source of low level venting. Chemosynthetic faunal associations together with population densities may be used to establish levels of fluid activity that directly affect slope stability (Tappin et al., 2001).
We conclude therefore that offshore surveying is an essential aspect of any assessment of areas considered under threat from tsunami attack. There are few case histories at present and PNG is probably one of the best studied to date. There is however often a great deal of offshore data that was acquired for other purposes and that can be utilized in assessing tsunami hazard. Use of these databases enables scientists to focus their future efforts on areas that are most tsunami prone. More focussed studies are then required to identify specific tsunami generation scenarios. Under such circumstances, mass failure and tsunami prediction are only one step away. Simultaneously, we also need to develop cost-effective tsunami mitigation strategies.

ACKNOWLDEGEMENTS

The authors wish to express their great appreciation to Alf Simpson, Director of SOPAC, who initiated the PNG offshore surveys and to JAMSTEC for providing the survey vessels and the funding for the authors' participation. One of the authors (PW) received partial research support from the US National Science Foundation. We also wish to thank all of our shipboard colleagues for the intense and valuable discussion on the possible sources of the 1998 tsunami. Lastly, we dedicate this paper to the people of Papua New Guinea, especially those who suffered from the tsunami attack. The data acquired following the disaster may help in their understanding of this devastating event. In the longer term, it may help others to withstand future tsunami attacks. DRT publishes with the permission of the British Geological Survey, Natural Environment Research Council, United Kingdom.

REFERENCES

Cooper, P. & B. Taylor 1987. Seismotectonics of New Guinea: a model for arc reversal following arc-continent collision. *Tectonics*. 6: 53-57

Crowhurst, P.V., K.C. Hill, D.A. Foster, & A.P. Bennett 1996. Thermochronological and geochemical constraints on the tectonic evolution of northern Papua New Guinea. In Hall, R and Blundell D., (eds) *Tectonic evolution of Southeast Asia, Geological Society Special Publication* 206: 525-537

Dugan, B. & P.B. Flemings 2000. Overpressure and Fluid Flow in the New Jersey Continental Slope: Implications for Slope Failure and Cold Seeps. *Science.* 289: 288-291.

Davies, H.L 1998. *The Sissano Tsunami 1998*. University of Papua New Guinea Printery, Port Moreseby. 48pp.

DeMets, C., R.G. Gordon, D.F. Argus, & Stein, S 1994. Effect of recent revisions to the geomagnetic reversal time scale. *Geophys. Res. Letts*. 21: 2191-2194.

Driscoll, N.W., J.K. Weissel & J. A. Goff 2000. Potential for large-scale submarine slope failure and tsunami generation along the U.S. mid-Atlantic coast. *Geology*. 28: 407-410.

Goldsmith, P., Barnett, A., Goff, J., McSaveny, M., Elliot, S. and Nongkas, M., 1999. Report of the New Zealand reconnaisance team to the area of the 17 July tsunami at Sissano Lagoon, Papua New Guinea. Bulletin of the New Zealand Society for Earthquake Engineering. 32. 102-118.

Kawata, Y., B.C. Benson, J.L. Borrero, H.L. Davies, W.P. de Lange, F. Imamura, H. Letz, J. Nott, & C. Synolakis 1999. Tsunami in Papua New Guinea was as intense as first thought. *Eos, Trans. Amer. Geophys. Union*. 80(9): 101,104-105

Matsumoto, T. C. Uechi & M. Kimura 1997. Surface deformation at the origin area of the 1771 Yaeyama Earthquake Tsunami observed by the precise survey off Yaeyama districts, Ryukyu area. *JAMSTEC J. Deep Sea Res*. 13:535-561.

McSaveny, M.J., Goff, J.R., Darby, D.J., Goldsmith, P., Barnett, A., Elliot, S., & M. Nongkas, 2000. The 17 July 1998 tsunami, Papua New Guinea: Evidence and initial interpretation. *Mar. Geol.* 170: 81-92.

Newman, A. V. & E.A. Okal, 1998 Moderately Slow Character of the July 17, 1998 Sandaun Earthquake as Studied by teleseismic Energy Estimates, (abs.), *Eos Trans. Amer. Geophys. Union.* 79, Fall Meeting. Supplement F564.

Orange, D.L.C., G.H. Greene, D. Reed, J.B. Martin, W.B.F. Ryan, N. Maher, D. Stakes, & J. Barry 1999. Widespread fluid expulsion on a translational continental margin: Mud volcanoes, fault zones, headless canyons, and organic-rich substrate in Monterey Bay, California. *Geol. Soc. Amer. Bull*. 111: 992-1009.

Okal, E. A. 1999. The probable source of the 1998 Papua New Guinea tsunami as expressed in oceanic T waves. Eos, 80, F750 (abstract).

Schwab, W.C., Lee, H.J. & D.C. Twichell 1993. Submarine landslides: Selected studies in the US exclusive economic zone. *Bull. U.S. Geol. Surv.* 2002, U.S., Dept. of Interior, Washington, D.C.

Sweet, S. & Silver, E. A. 2002. Tectonics and slumping in the source region of the 1998 Papua New Guinea tsunami from seismic reflection images. Submitted.

Stevens, C., R. McCaffrey, E.A. Silver, Z. Sombo, P. English, & J. van der Kevie 1998. Mid-crustal detachment and ramp faulting in the Markham Valley, Papua New Guinea. *Geology*. 26: 847-850.

Tappin, D.R., T. Matsumoto, & shipboard scientists. 1999. Offshore Surveys Identify Sediment Slump as Likely Cause of Devastating Papua New Guinea Tsunami 1998. *Eos Trans. Amer Geophys Union.* 80(30): 329, 334, 340.

Tappin, D.R., P. Watts, G. M. McMurtry, Y. Lafoy & T. Matsumoto, 2001. The Sissano, Papua New Guinea tsunami of July 1998– offshore evidence on the source mechanism. *Mar. Geol.* 175: 1-23.

Titov, V. & F. Gonzalez, 1998. Numerical study of the source of the July 1998 PNG earthquake (abs.), *Eos Trans. Amer. Geophys. Union*, 79, Fall Meeting. Supplement. F564,

Tregoning, P., K. Lambeck, A. Stolz, P. Morgan, S.C. McCluskey, P. van der Beek, H. McQueen, R.R. Jackson, R.P. Little, A. Laing, & B. Murphy. Estimation of current plate motions in Papua New Guinea from Global Positioning System observations. *Jour. Geophys*. *Res*. 103: 12181-12203.

Turner, A. K., & R.L. Schuster 1996. Landslides: Investigation and mitigation. Special Report 247, *Trans. Res. Board*, National Academy Press, Washington, D.C

von Huene, R., & D.W. Scholl 1991. Observations at convergent margins concerning sediment subduction, subduction erosion, and the growth of continental crust. *Rev. Geophys.*, 29, 279-316.

von Heune, R., D. Klaeschen & J. Fruehn 1999. Relation between the Subducting Plate and Seismicity Associated with the Great 1964 Alaska Earthquake. In. J. Sauber and R. Dmowska (eds), *Seismogenic and tsunamigenic processes in shallow subduction zones*. PAGEOPH Volume 154(3/4): 575-592.

von Heune, R., J. Corvalan, E.R. Flueh, K. Hinz, J. Korstgard, C.R. Ranero, W. Weinrebe & CONDOR Scientists 1997. Tectonic control of the subducting Juan Fernandez Ridge on the Andean margin near Valparaiso, Chile. *Tectonics*. 16: 474-488.

Watts, P. & J. C. Borrero 2001. Probability distributions of landslide tsunamis. Proceedings of the International Tsunami Symposium 2001, Seattle, WA, 697-710.

Watts, P., J.C. Borrero, D.R. Tappin, J.-P. Bardet, S.T. Grilli & C.E. Synolakis 2002. Novel simulation technique employed on the 1998 Papua New Guinea tsunami. Presented at the 1999 IUGG General Assembky in Birmingham, U.K. and published by the first author at *www.appliedfluids.com/resume.html/*.

Watts, P. & S.T. Grilli, (submitted). Tsunami generation by submarine mass failure I: Wavemaker models. *Journ. Watrwy. Port., Coast. & Ocean Eng*. ASCE..